Section 2   Plasma Physics

Chapter 1   Plasma Dynamics

Chapter 1. Plasma Dynamics

Academic and Research Staff

Professor Abraham Bers, Professor Bruno Coppi, Dr. Stefano Migliuolo, Dr. Abhay K. Ram, Dr. Linda E. Sugiyama

Visiting Scientists and Research Affiliates

Dr. Didier Benisti,[1] Dr. Giuseppe Bertin, Dr. Francesca Bombarda, Dr. Madhurjya Bora, Dr. Vladimir Fuchs,[2] George M. Svolos, Dr. Joachim Theilhaber[3]

Graduate Students

Vitali Belevtsev, William S. Daughton, Darin R. Ernst, Ronald J. Focia, Gregory E. Penn, Ante Salcedo, Steven D. Schultz, Kenneth C. Wu

Undergraduate Students

Ilija Jergovic, Peter P. Ouyang, Evan H. Reich

Technical and Support Staff

Laura M. von Bosau

1.1 Plasma Wave Interactions—RF Heating and Current Generation

1.1.1 Introduction

The research of this group is concerned with both basic and applied problems in the electrodynamics of plasmas. Basic to the electrodynamics of plasmas are interactions of various plasma waves with the constituent charged particles of the plasma, as well as interactions between different plasma waves. These interactions are generally nonlinear and entail studies of the evolution of coherent structures (e.g., solitons) as well as chaotic dynamics (low-dimensional and spatiotemporal chaos). Applied studies of current interest address problems in magnetic confinement fusion, space plasma physics, and inertial confinement fusion. In particular, we study (1) RF heating and current drive in magnetically confined plasmas, (2) the energization of O^+ and H^+ ions from the ionosphere to the magnetosphere, and (3) light scattering instabilities in laser-plasma interactions.

In the following, we summarize our significant progress on five projects. The first report (1.1.2) relates to our proposal on heating and current drive with electron Bernstein waves (EBW) at the National Spherical Torus Experiment, a national facility for studying high-β plasmas in low aspect ratio tokamaks. In particular, we report on a new analysis of the mode conversion process for coupling external electromagnetic power to the kinetic EBW in the plasma. The second and third reports (1.1.3 and 1.1.4) describe ongoing work following our discovery last year of a new nonlinear mechanism for coherent and chaotic acceleration of ions. Specifically, we are pursuing two applications for this mechanism: (1) understanding some of the observed ion acceleration from the ionosphere to the magnetosphere, and (2) proposing new means of plasma heating with two (or more) lower-hybrid waves. The fourth report (1.1.5) describes our continuing work on the interaction of the intrinsic tokamak bootstrap current with externally RF drive current for achieving a steady-state tokamak operation; we report on our progress in developing coupled velocity and configuration space codes for these studies. The last report (1.1.6) initiates a new study of laser-plasma interactions of interest to inertial confinement fusion; in particular, we show first results on the three-dimensional space and time evolution of laser-plasma instabilities in such interactions.

---

1   Consorzio RFX, Corso Stati Uniti, Padova, Italy.

2   Centre Canadien de Fusion Magnétique (CCFM), Québec, Canada.

3   Whitehead Institute, MIT Center for Genome Research, Cambridge, Massachusetts.

1.1.2 Coupling to Electron Bernstein Waves in High-β Tokamaks

Sponsors

Project Staff

Professor Abraham Bers, Dr. Abhay K. Ram, Steven D. Schultz

In *Progress Report* No. 139, we showed that a triplet mode conversion scenario (cutoff-resonance-cutoff) exists for coupling from an X-mode to an electron Bernstein wave (EBW) in tokamaks.[4] This is of particular interest to high-β tokamaks, such as the planned National Spherical Torus Experiment (NSTX), in which EBW could be used for plasma heating and current drive.

In this report, we present analyses on the excitation of EBWs from the outboard side by either mode conversion of an X-mode or its direct coupling in an NSTX-type of plasma. Figure 1 shows the distribution of critical frequencies in propagation across the magnetic field along the equatorial plane, and Figure 2 gives the local kinetic dispersion relation for the same direction; both use the plasma (density and temperature) and magnetic field profiles (Figure 3) for a calculated equilibrium in NSTX.[5] From Figure 1 and Figure 2, we note that the triplet of R-cutoff—upper-hybrid-resonance (UHR)—L-cutoff forms a mode conversion resonator (i.e., a resonator containing mode conversion to EBW as an effective dissipa-

tion).[6] In such a triplet resonator, one can, in principle, obtain complete mode conversion of the incident power to EBW.[7]
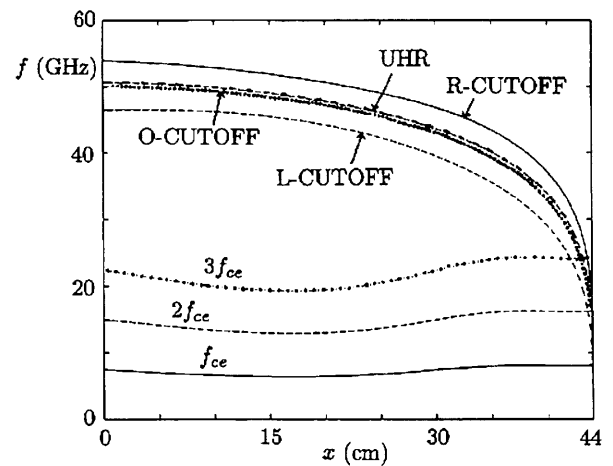

Figure 1. Distribution of critical frequencies in propagation across the magnetic field along the equatorial plane in NSTX (Figure 3).[8]

We consider first the simplest cold-plasma slab model in the equatorial plane, inhomogeneous in x (the radial direction), and with arbitrary x-variations for both the (toroidal) z-directed and the (poloidal) y-directed magnetic fields: $\vec{B}_0(x) = \hat{y}B_p(x) + \hat{z}B_t(x)$. The detailed linearized field analysis is straightforward. For numerically integrating the field equations, it is found convenient to formulate them as a set of four coupled first-order differential equations:

$$\frac{d\vec{F}_c}{d\xi} = i\overleftrightarrow{A}_c \cdot \vec{F}_c \tag{1}$$

4   A. Bers, A.K. Ram, D. Benisti, V. Fuchs, J. Theilhaber, R.J. Focia, F.W. Galicia, S.D. Schultz, L. Vacca, and K.C. Wu, "Plasma Wave Interactions—RF Heating and Current Generation," *MIT RLE Progress Report* 139: 243-46 (1996).

5   NSTX parameters (courtesy of R. Majeski, Princeton Plasma Physics Laboratory): R = 1.05 m, a = 0.44 m; $n_{e0} = n_E + (n_0 - n_E)$ $(1 - x^2 / a^2)^{1/2}$; $n_0 = 4 \times 10^{19} / m^3$; $T_{e0} = T_E + (T_0 - T_E)$ $(1 - x^2 / a^2)^2$; $T_0 = 3$ keV; $(n_E, T_E) = 0.02$ (n_0, T_0).

6   V. Fuchs, A.K. Ram, S.D. Schultz, A. Bers, and C.N. Lashmore-Davies, "Mode Conversion and Electron Damping of the Fast Alfvén Wave in a Tokamak at the Ion-Ion Hybrid Frequency," *Phys. Plasmas* 2: 1637 (1995); A.K. Ram, A. Bers, S.D. Schultz, and V. Fuchs, "Mode Conversion of Fast Alfvén Waves at the Ion-Ion Hybrid Resonance," *Phys. Plasmas* 3: 1976 (1996); A. Bers, A.K. Ram, A. Bécoulet, and B. Saoutic, "Theory of Plasma Resonator with Mode Conversion Absorption," *Phys. Plasmas*, forthcoming.

7   K.C. Wu, A.K. Ram, A. Bers, and S.D. Schultz, "Electron Cyclotron Heating in NSTX," *Proceedings of the 12th Topical Conference on Radio Frequency Power in Plasmas*, Savannah, Georgia, April 1-3, 1997, eds. P.M. Ryan and T. Intrator (New York: American Institute of Physics) Conference Proceedings 403: 207-10, 1997.

8   NSTX parameters (courtesy of R. Majeski, Princeton Plasma Physics Laboratory): R = 1.05 m, a = 0.44 m; $n_{e0} = n_E + (n_0 - n_E)$ $(1 - x^2 / a^2)^{1/2}$; $n_0 = 4 \times 10^{19} / m^3$; $T_{e0} = T_E + (T_0 - T_E)$ $(1 - x^2 / a^2)^2$; $T_0 = 3$ keV; $(n_E, T_E) = 0.02$ (n_0, T_0).
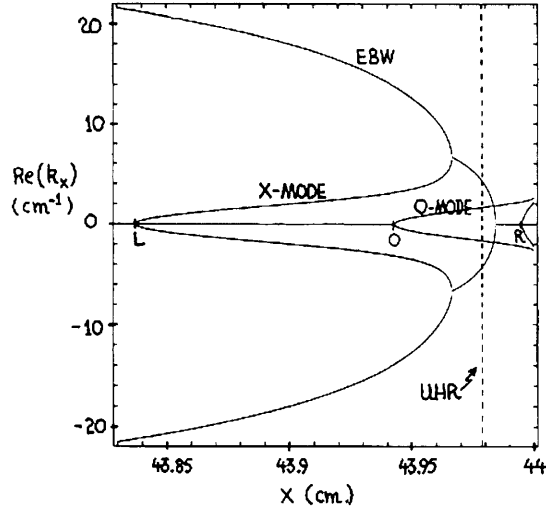
Figure 2. Local kinetic dispersion relation for the same parameters as in Figure 1.
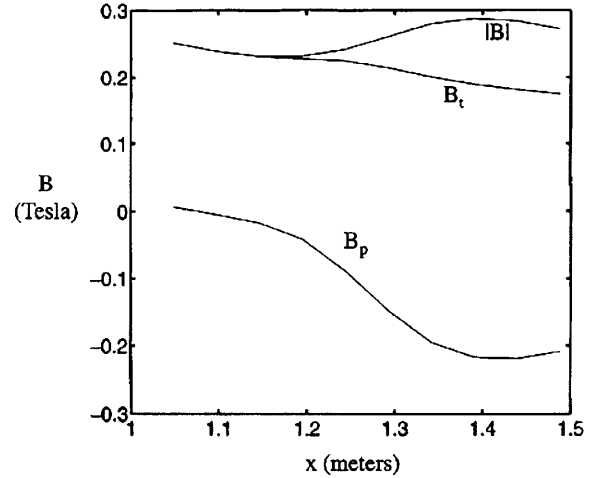

Figure 3. Magnetic field profiles in NSTX (courtesy R. Majeski).

where $\vec{F}_c^T = [E_y \ E_z \ (-cB_y) \ cB_z]$, we have let $(\omega x / c) \equiv \xi$, and the variations in the directions y and z (in which the equilibrium is assumed uniform) have been Fourier analyzed with components, respectively, $\exp(ik_y y)$ and $\exp(ik_z z)$. The matrix $\overleftrightarrow{A}_c$ is found to be given by

$$
\overleftrightarrow{A}_c = \frac{1}{K_{xx}} \begin{bmatrix} -n_y \chi_{xy} & -n_y \chi_{xz} & -n_y n_z & K_{xx} - n_y^2 \\ -n_z \chi_{xy} & -n_z \chi_{xz} & K_{xx} - n_z^2 & -n_y n_z \\ K_{xx}(\chi_{yz} + n_y n_z) + \chi_{xy}\chi_{xz} & K_{xx}(K_{zz} - n_y^2) + \chi_{xz}^2 & n_z \chi_{xz} & n_y \chi_{xz} \\ K_{xx}(K_{yy} - n_z^2) + \chi_{xy}^2 & K_{xx}(\chi_{yz} + n_y n_z) + \chi_{xy}\chi_{xz} & n_z \chi_{xy} & n_y \chi_{xy} \end{bmatrix}
\tag{2}
$$

where $n_y = (ck_y/\omega)$, $n_z = (ck_z/\omega)$, and the susceptibility χ_{ij} and permitivity $K_{ij} = \delta_{ij} + \chi_{ij}$ elements are as found from standard cold plasma perturbation theory for the considered equilibrium $\vec{B}_0(x)$ and $n_0(x)$. The solid line curve in Figure 4 shows the mode conversion/resonant absorption as a function of frequency, obtained from a numerical integration of (1) for NSTX plasma and magnetic field profiles, assuming $n_y = 0$ and $n_z = 0.1$. We note that high-mode conversion efficiencies, >80%, are obtained over a broad range of frequencies of about 4 GHz around the peak in $C \approx 0.97$ at f = 16 GHz.

Accounting for kinetic effects in a nonzero temperature plasma removes the resonant absorption at the UHR and replaces it with the kinetic EBW, which propagates the energy away from the mode conversion region. An approximate description that includes the kinetic EBW and the cold plasma modes, coupled near the UHR, follows from general WKB analysis,[9] with due attention to conservation of kinetic energy flow density. Thus to include the EBW, we set

$$
K_{xx}^K E_x \rightarrow K_{xx} E_x - \frac{d}{d\xi}\left(T \frac{dE_x}{d\xi}\right).
\tag{3}
$$

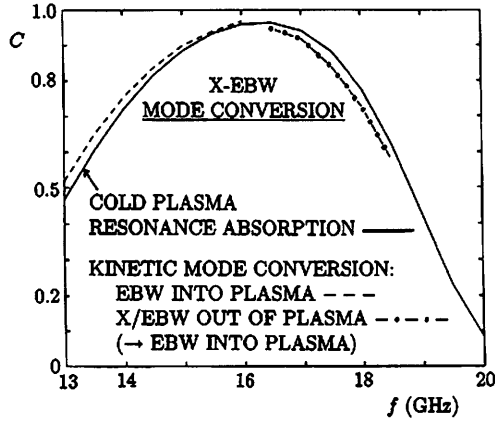9   H. Berk and D.L. Book, "Plasma Wave Regeneration in Inhomogeneous Media," *Phys. Fluids* 12: 649 (1969).

Figure 4. X-EBW mode conversion as a function of frequency.

Here

$$T = \frac{-3\omega_p^2\omega^2(\upsilon_T/c)^2}{(\omega^2 - \omega_{ce}^2)(\omega^2 - 4\omega_{ce}^2)} \tag{4}$$

is obtained from expanding the kinetic (Vlasov) susceptibility χ_{xx}^K to second-order in $(k_\perp v_{Te}/\omega_{ce})$. This is appropriate for representing EBW between the first and second electron cyclotron harmonics and where damping can be neglected. The resulting set of coupled first-order differential equations are

$$\frac{d\vec{F}_k}{d\xi} = i\overset{\leftrightarrow}{A}_K \cdot \vec{F}_K \tag{5}$$

where $\vec{F}_K^T = [E_x \; E_y \; E_z(iTE'_x) \; cB_z \; (-cB_y)]$, we have let $(\omega x/c) \equiv \xi$,

$$\overset{\leftrightarrow}{A}_K = \begin{bmatrix} 0 & 0 & 0 & -T^{-1} & 0 & 0 \\ n_y & 0 & 0 & 0 & 1 & 0 \\ n_z & 0 & 0 & 0 & 0 & 1 \\ K_{xx} & \chi_{xy} & \chi_{xz} & 0 & n_y & n_z \\ -\chi_{xy} & K_{yy}-n_z^2 & \chi_{yz}+n_yn_z & 0 & 0 & 0 \\ -\chi_{xz} & \chi_{yz}+n_yn_z & K_{zz}-n_y^2 & 0 & 0 & 0 \end{bmatrix} \tag{6}$$

The dashed and dot-dashed curves in Figure 4 show the results from a numerical integration of (5) for the same NSTX parameters used in the mode-conversion/resonance absorption calculations given above. The approximate kinetic mode-conversion calculation is seen to verify very well the results from the exact mode-conversion/resonance absorption calculation. For frequencies below 16 GHz (dashed curve), the upper-hybrid frequency is between the first and second harmonics of the electron cyclotron frequency and the kinetic EBW carries the power into the plasma. For frequencies above 16 GHz (dot-dashed curve), the upper-hybrid frequency is just above the second harmonic of the electron cyclotron frequency, and, unless the plasma extends sufficiently out, the power incident on the fast X-mode will only encounter a forward travelling wave (modified slow X-mode/EBW) propagating out of the plasma; otherwise this can also be expected to convert to an EBW carrying power into the plasma. This latter case is now under study. The important result is that calculations of the power mode-converted based upon a model that accounts for the kinetic nature of the EBW are essentially the same as the ones based upon resonance absorption in a cold plasma. The importance of accounting for kinetic effects is to obtain the correct energy flow of the EBW.

Turning to direct coupling to EBW, we note from Figure 1 and Figure 2 that for plasma parameters of interest and frequencies not too far above f_{ce}, the distances at the plasma edge over which coupling takes place are shorter than a free-space wavelength. This suggests that effective direct coupling to EBW should be possible from an external slow-wave structure that can be placed just inside of the confluence point of the EBW with the slow X-mode. This coupling problem, which is similar to slow-wave coupling for lower-hybrid and ion-Bernstein waves, is currently under study.

1.1.3 Energization of Ionospheric Ions by Lower Hybrid Waves

Sponsor

Project Staff

Dr. Abhay K. Ram, Professor Abraham Bers, Dr. Didier Benisti

In *Progress Report* No. 139 we described a new phenomenon of nonlinear coherent energization by multiple electrostatic waves.[10] The details of the nonlinear coherent energization process and the energization to high energies by electrostatic waves has been the subject of some of our recent publications.[11] This energization process is useful in explain-

ing the transverse (to the geomagnetic field) energization of ionospheric oxygen O^+ and hydrogen H^+ ions in the auroral ionosphere of the earth.

Observations

Our analysis is aimed at understanding specific observations reported by Kintner[12] and by Vago.[13] The observations from the Topaz 3 rocket, which was launched northward from Poker Flats, Alaska, in 1991, show that, at altitudes near 1000 km, there is transverse (to the geomagnetic field) energization of auroral ionospheric ions in localized regions of intense lower hybrid waves. The energization occurs in density-depleted regions of about 50-100 m across the geomagnetic field $\vec{B}$ (and ~100 km along $\vec{B}$)[14] within which exist intense electric fields ranging in amplitude from 50 to 150 mV/m. Within these regions, the oxygen O^+ and hydrogen H^+ ions are observed to be accelerated transversely with characteristic energies in the range 6-10 eV. The ambient energies of the ions in this part of the ionosphere is approximately 0.34 eV (corresponding to a plasma temperature of 4000 K). Observations show that, predominantly, the bulk of the H^+ distribution is energized, while for O^+ the tail distribution gets energized. Occasionally, the tail of the H^+ distribution displayed transverse energization. The H^+ ions are the minority ion species with the ambient density of O^+ being larger than the H^+ density by about an order of magnitude. The wave spectrum, observed to be cutoff near the local lower hybrid frequency, ranges in frequency from about 5 kHz to about 12 kHz. These lower hybrid waves are primarily coherent, electrostatic, propagating across the geomagnetic field, and ranging in wavelengths from 2 m to 20 m. Very importantly, from a theoretical point of view, the Topaz 3 observations showed that the lower hybrid waves are inducing transverse energization of ions; the ions are not responsible for the generation of these field structures comprised of lower hybrid

waves. The generation and the physical mechanisms responsible for these lower hybrid structures is presently not very well understood.

Modeling the Motion of Ions

Within the context of the above observations, our aim is to understand the energization of ionospheric ions inside the lower hybrid field structures. Toward this end, we will assume, consistent with observations, that the lower hybrid waves lead to the energization of ions through wave-particle interactions. Since the ions are not responsible for the generation and presence of the structures with enhanced lower hybrid electric field amplitudes, we will study the dynamics of ions in prescribed electrostatic fields whose characteristic properties are similar to those observed by Topaz 3.

The motion of an ion interacting with N plane electrostatic waves, propagating perpendicularly (along $\hat{x}$ to an ambient uniform magnetic field $\vec{B} = B_0\hat{z}$, is given by

$$\frac{dx}{dt} = v \tag{7}$$

$$\frac{dv}{dt} = -\Omega^2 x + \sum_{i=1}^{N} \frac{QE_i}{M} \sin(k_i x - \omega_i t) \tag{8}$$

where x and v are the position and velocity of an ion of charge Q and mass M, respectively, E_i is the electric field amplitude of the ith plane wave with wavenumber k_i and angular frequency ω_i, and $\Omega = QB_0/M$ is the ion cyclotron frequency. The Hamiltonian corresponding to equations (7) and (8) is

10 A. Bers, A.K. Ram, D. Benisti, V. Fuchs, J. Theilhaber, R.J. Focia, F.W. Galicia, S.D. Schultz, L. Vacca, and K.C. Wu, "Plasma Wave Interactions—RF Heating and Current Generation," *MIT RLE Progress Report* 139: 233-47 (1996).

11 D. Benisti, A.K. Ram, and A. Bers, "New Mechanisms of Ion Energization by Multiple Electrostatic Waves in a Magnetized Plasma," *Phys. Rev. Lett.*, forthcoming; D. Benisti, A.K. Ram, and A. Bers, "Ion Dynamics in Multiple Electrostatic Waves in a Magnetized Plasma. Part I: Coherent Acceleration," submitted to *Phys. Plasmas*; D. Benisti, A.K. Ram, and A. Bers, "Ion Dynamics in Multiple Electrostatic Waves in a Magnetized Plasma. Part II: Enhancement of the Acceleration," submitted to *Phys. Plasmas*; A.K. Ram, A. Bers, and D. Benisti, "Ionospheric Ion Acceleration by Multiple Electrostatic Waves," *J. Geophys. Res.*, forthcoming.

12 P.M. Kintner, J. Vago, S. Chesney, R.L. Arnoldy, K.A. Lynch, C.J. Pollock, and T.E. Moore, "Localized Lower Hybrid Acceleration of Ionospheric Plasma," *Phys. Rev. Lett.* 68: 2448 (1992).

13 J.L. Vago, P.M. Kintner, S.W. Chesney, R.L. Arnoldy, K.A. Lynch, T.E. Moore, and C.J. Pollock, "Transverse Ion Acceleration by Localized Lower-Hybrid Waves in the Topside Auroral Ionosphere," *J. Geophys. Res.* 97: 16935 (1992).

14 R. Arnoldy, K. Lynch, P. Kintner, J. Vago, C.J. Pollock, and T.E. Moore, "Transverse Ion Acceleration and Auroral Electron Precipitation," *Adv. Space Res.* 13: 143 (1993).

$$H(x, v, t) = \frac{1}{2}(v^2 + \Omega^2 x^2) + \sum_{i=1}^{N} \frac{QE_i}{Mk_i} \cos(k_i x - \omega_i t) \quad (9)$$

which can be expressed in terms of the normalized action-angle variables of the unperturbed ($E_i = 0$ for all i) system

$$H(\psi, I, \tau) = I + \sum_{i=1}^{N} \frac{\varepsilon_i}{k_i} \cos\{k_i \sqrt{2I}\sin(\psi) - \nu_i \tau\} \quad (10)$$

$$= I + \sum_{i=1}^{N} \frac{\varepsilon_i}{k_i} \sum_{n=-\infty}^{\infty} J_n(k_i \sqrt{2I})\cos(n\psi - \nu_i \tau)$$

where we have replaced k_i/k_1 by k_i,

$I = [(k_1 x)^2 + (k_1 v/\Omega)^2]/2 = \rho^2/2$ and

$\psi = \tan^{-1}(x\Omega/v)$ are the normalized action and angle variables, respectively, ρ is the normalized Larmor radius of the ion, $\varepsilon_i = QE_i k_i/(M\Omega^2)$, $\nu_1 = \omega_i/\Omega$, and $\tau = \Omega t$. The action I is a measure of the energy of an ion. In order to provide a feeling for the normalized quantities, consider a singly charged O^+ ion with an initial ambient energy of 0.34 eV, in a magnetic field $B_0 = 0.36$ G, interacting with a single wave of amplitude 100 mV/m, frequency 5 kHz, and wavelength 2 m, corresponding to the lowest measured phase velocity with substantial electric field amplitude. Then $I \approx 220.7$, $\rho \approx 21$, $\varepsilon \approx 40.7$, and $\nu \approx 146.2$ where we have dropped the subscripts on ε and ν. For a H^+ ion with an energy of 0.34eV, the corresponding values would be $I \approx 13.8$, $\rho \approx 5.3$, $\varepsilon \approx 2.55$, and $\nu \approx 9.1$.

Interaction With a Single Electrostatic Wave

There have been a number of studies on the effect of a single wave on the dynamics of an ion.[15] These studies have been applied to understanding wave-particle interactions in space plasmas.[16] The need to study the dynamics of O^+ and H^+ ions in more than one electrostatic wave is clearly demonstrated by the results obtained from these previous studies. In general, it has been found that an ion gains energy from a single wave only if its motion becomes chaotic.[17] Otherwise, on the average, an ion will not gain any energy. The ion motion becomes chaotic if the wave amplitude is above a threshold value:[18]

$$\varepsilon > \varepsilon_{th} \approx \frac{1}{4}\nu^{2/3} \quad (11)$$

and if the initial values of the normalized Larmor radius ρ_0 of the ion are within the following bounds:[19]

$$\nu - \sqrt{\varepsilon} \lesssim \rho_0 \lesssim \left(\frac{2}{\pi}\right)^{1/3} (4\varepsilon\nu)^{2/3} \quad (12)$$

The left-hand side of the above inequality gives the lower bound, in ρ, of the chaotic phase space, and the right-hand side gives the upper bound. For an ion to get energized by its interaction with a single wave, its ρ_0 has to be within the bounds given by (12). Otherwise, the ion will not gain any energy and its motion will remain coherent.

If we consider a wave with frequency 5 kHz and wavelength 2 m in a magnetic field of 0.36 G, then the threshold amplitude for chaotic motion is

$$\varepsilon_{th}^O \approx 6.94 \Rightarrow E_{th}^O \approx 17.0 \text{mV/m} \quad (13)$$

$$\varepsilon_{th}^H \approx 1.1 \Rightarrow E_{th}^H \approx 2.9 \text{mV/m}$$

for O^+ and H^+, respectively. Since the electric field amplitudes in the structures observed by Topaz 3 are well above these threshold values, part of the phase space of O^+ and H^+ will be chaotic. The chaotic region of phase space, obtained from (12) for an electric field amplitude of 100 mV/m, for O^+ and H^+ is

$$139.8 \leq \rho_0^O \leq 712.2 \Rightarrow 15.3 \text{eV} \leq I_0^O \leq 396.1 \text{eV}$$

$$7.5 \leq \rho_0^H \leq 17.7 \Rightarrow 0.7 \text{eV} \leq I_0^H \leq 3.9 \text{eV}$$

$$(14)$$

15 A. Fukuyama, H. Mometa, R. Itatani, and T. Takizuka, "Stochastic Acceleration by an Electrostatic Wave Near Ion Cyclotron Harmonics," *Phys. Rev. Lett.* 38: 701 (1977); C.F.F. Karney and A. Bers, "Stochastic Ion Heating by a Perpendicularly Propagating Electrostatic Wave," *Phys. Rev. Lett.* 39: 550 (1977); C.F.F. Karney, "Stochastic Ion Heating by a Lower Hybrid Wave," *Phys. Fluids* 21: 1584 (1978).

16 K. Papadopoulos, J.D. Gaffey, Jr., and P.J. Palmadesso, "Stochastic Acceleration of Large *m/q* Ions by Hydrogen Cyclotron Waves in the Magnetosphere," *Geophys. Res. Lett.* 7: 1014 (1980); R.L. Lysak, "Ion Acceleration in the Magnetosphere and Ionosphere," in *Geophys. Monogr. Ser.* 38: 261-70, ed. T. Chang (Washington, District of Columbia: American Geophysical Union, 1986).

17 C.F.F. Karney and A. Bers, "Stochastic Ion Heating by a Perpendicularly Propagating Electrostatic Wave," *Phys. Rev. Lett.* 39: 550 (1977); C.F.F. Karney, "Stochastic Ion Heating by a Lower Hybrid Wave," *Phys. Fluids* 21: 1584 (1978).

18 Ibid.

19 Ibid.

respectively, where the units of I_0 have been re-expressed in terms of energy. In Figure 5, we plot this chaotic part of phase space in energy units for O^+ and H^+ and show the range of energies for these ions as observed by Topaz 3. The problems associated with explaining the observed energy ranges of O^+ and H^+ using a single-wave model are now readily apparent. The lower bound of the O^+ chaotic phase space is at about 50 times the ambient thermal energy of O^+, and hence encompasses a negligible number of O^+ ions. Furthermore, the entire chaotic region for O^+ is well above the observed O^+ energies. The maximum energy of the chaotic region is much larger than the observed energy range for the energized O^+ ions. So even if it were possible to extend the lower part of the O^+ chaotic space into the O^+ thermal distribution function, the energies that O^+ ions could achieve would be significantly larger than the observed energy range. For H^+ ions the problem is a bit different. The lower part of the H^+ chaotic region is at about twice the ambient thermal energy of H^+. So a significant population of H^+ ions have access to the chaotic phase space. However, the maximum energy that these ions can achieve is well below the observed energy range.
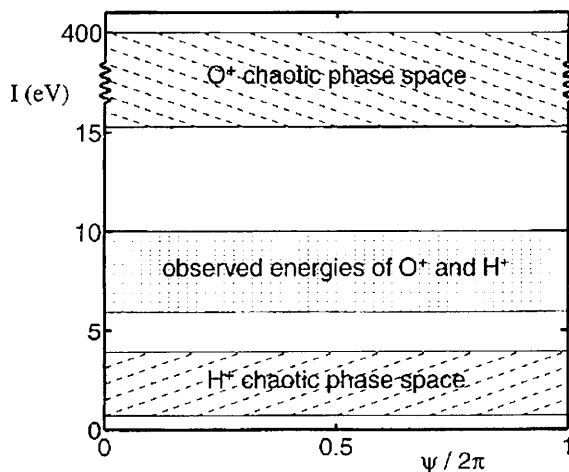

Figure 5. The chaotic part of phase space of H^+ and O^+ ions as obtained from a single-wave analysis. The single wave is assumed to have a wavelength of 2 m, a frequency of 5 kHz, and an amplitude of 100 mV/m. Also shown is the observed range of ion energies.

Coherent Energization in a Broadband Spectrum

In the last *Progress Report*,[20] we described the nonlinear coherent energization that occurs when low-energy ions interact with two waves that are separated in frequency by an integer (≤ 3) multiple of the ion cyclotron frequency. The results obtained from this study are a useful guide for determining some of the necessary conditions for which coherent energization can occur in a broadband spectrum of waves. We find that a necessary criterion for coherent energization in a broadband spectrum of waves is that the spectrum has to be composed of pairs of waves that are separated by an ion cyclotron frequency; each pair could be randomly distributed in frequency with respect to any other pair. Numerical simulations for a variety of frequencies and frequency bandwidths confirm this necessary criterion.

Application to O^+ Energization

In order to estimate the time it would take O^+ ions to get energized by nonlinear coherent energization to 10 eV in a broadband spectrum of waves of the sort observed by Topaz 3, we consider the dynamics in a spectrum of 162 waves ranging in frequency from $146.2\Omega_0$ to $200\Omega_0$ (Ω_0 is the O^+ cyclotron frequency), corresponding to a range from 5 kHz to 6.84 kHz. All of the waves are assumed to have the same wavelength of 2 m and the same amplitude of 25 mV/m. The root mean square amplitude of the electrostatic field is approximately 225 mV/m. The result for two O^+ ions started at different initial energies is plotted in Figure 6. Ion 1 is initially at a transverse energy of approximately 2.3 eV (corresponding to a transverse speed of about 2.6 times the thermal speed), and ion 2 is initially at a transverse energy of approximately 4.6 eV (corresponding to a transverse speed of about 3.6 times the thermal speed). (Since observations show that the tail of the O^+ distribution function is energized, we have chosen these initial O^+ ion energies as representative of the tail ions.)

From Figure 6, we find that the time needed for ions 1 and 2 to be transversely energized to 10 eV (the dashed line in Figure 6) is $\tau_E{}^1 \sim 122s$ and $\tau_E{}^2 \sim 65s$, respectively. The simulation result shows that both of the O^+ ions will make it into the chaotic region of phase space which exists at higher energies. The time taken to reach the chaotic region is about 153 s

20   A. Bers, A.K. Ram, D. Benisti, V. Fuchs, J. Theilhaber, R.J. Focia, F.W. Galicia, S.D. Schultz, L. Vacca, and K.C. Wu, "Plasma Wave Interactions—RF Heating and Current Generation," *MIT RLE Progress Report* 139: 233-47 (1996).

and 88 s, respectively, for the two ions. However, in order to reach the observed energies of 10 eV, the O⁻ ions have to be energized by the nonlinear coherent mechanism discussed in our previous *Progress Report*.[21]
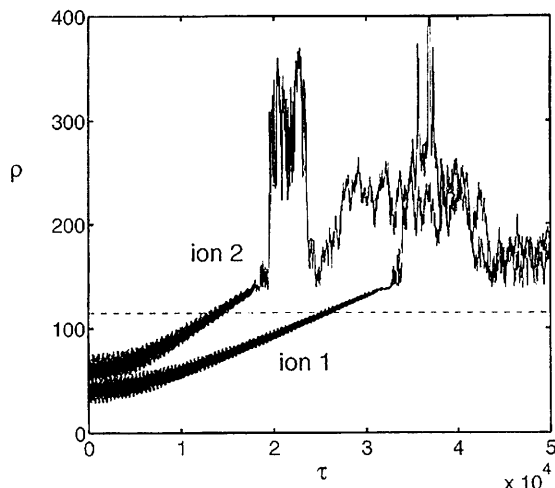

Figure 6. The dynamics of two ions in 162 waves. All the waves have the same normalized wavenumber $k_i = 1$ and normalized amplitude $\varepsilon_i = 10.7$, for i = 1,2,...,162. The frequencies of these waves are $v_{3n-2} = 146.2+n$, $v_{3n-1} = 146.381+n$, $v_{3n} = 146.873+n$, for n = 1,2,...,54. The wavelength and the electric field amplitude of each wave are 2 m and 25 mV/m, respectively. Initially ion 1 has $\rho_0^{(1)} = 54$, corresponding to an energy of 2.3 eV, and ion 2 has $\rho_0^{(2)} = 76.5$, corresponding to an energy of 4.6 eV. Both ions start off with an initial phase $\psi_0 = 0$.

It is worth comparing the energization time τ_E with some other timescales that are relevant to this problem. At an altitude of 1000 km, and assuming the geomagnetic field to be 0.36 G, the gyrocenter of an O⁺ ion, with a parallel energy of 1/3 eV and a perpendicular energy of 10 eV, drifts transversely owing to the gradient and curvature of the geomagnetic field[22] at a speed of about 9×10^{-3}m/s. In the time it takes the two ions to get energized to 10 eV, their gyrocenters have drifted by about 1.1 m and 0.6 m, respectively. This drift is significantly less than the transverse width of the lower hybrid structures observed by Topaz 3. So the ions would not drift out of the interaction region within the time it takes to get transversely

energized to 10 eV. If we assume that the speed along the geomagnetic field of the two ions is their thermal speed, then the distance traveled along the geomagnetic field by the two ions, before they get transversely energized to 10 eV, is approximately 173 km and 92 km, respectively. Thus the lower hybrid structures have to extend up to about 173 km and 92 km, respectively, along the geomagnetic field for the two ions to be transversely energized to 10 eV. These distances are comparable to the estimated lengths of the lower hybrid structures along the geomagnetic field which are of the order of a few hundred kilometers.[23] The fractional change in the strength of the geomagnetic dipolar field over a distance of 173 km is less than 0.01%. Thus our approximation of a constant magnetic field is very reasonable. These results indicate that the tail of the O⁺ distribution function is likely to get accelerated by the nonlinear coherent energization mechanism for reasonable sizes of the lower hybrid structures. Also, ions with initially small parallel velocities are more likely to get accelerated than those with larger parallel velocities.

The results in Figure 6 also show that the O⁺ ions can get energized beyond 10 eV and make it into the chaotic region where they can achieve much higher energies. However, the corresponding timescales are long which, in turn, implies that the required parallel length of the lower hybrid structures has to be larger than the length required to get to 10 eV.

1.1.4 Interaction of Ions With Two Lower Hybrid Waves in Tokamaks

Sponsor

U.S. Department of Energy
Grant DE-FG02-91-ER-54109

Project Staff

Dr. Abhay K. Ram, Professor Abraham Bers

The nonlinear coherent and chaotic energization processes by multiple electrostatic waves[24] can also be used as a new means of effective ion heating in magnetically confined plasmas. We have developed a possible scenario that takes advantage of the nonlin-

21 A. Bers, A.K. Ram, D. Benisti, V. Fuchs, J. Theilhaber, R.J. Focia, F.W. Galicia, S.D. Schultz, L. Vacca, and K.C. Wu, "Plasma Wave Interactions—RF Heating and Current Generation," *MIT RLE Progress Report* 139: 233-47 (1996).

22 L.R. Lyons and D.J. Williams, *Quantitative Aspects of Magnetospheric Physics* (Norwell, Massachusetts: D. Reidel, 1984), pp. 14-20.

23 R. Arnoldy, K. Lynch, P. Kintner, J. Vago, C.J. Pollock, and T.E. Moore, "Transverse Ion Acceleration and Auroral Electron Precipitation," *Adv. Space Res.* 13: 143 (1993).

ear coherent energization process for ion heating by two lower hybrid waves in laboratory tokamak plasmas.

The motion of an ion interacting with two-plane electrostatic waves is given by the following normalized equation:

$$\frac{d^2 x}{d\tau^2} + x = \varepsilon_1 \sin(x - v_1\tau) + \varepsilon_2 \sin(\kappa x - v_2\tau) \qquad (15)$$

To study the nonlinear coherent energization of ions in tokamaks, we have chosen parameters relevant to the Alcator C-Mod experiment at MIT. We have assumed a major radius of 0.67 m, a minor radius of 0.22 m, a peak density of $5\times10^{20}m^{-3}$, and a parabolic density profile. For a lower hybrid wave frequency of 2.45 GHz, if we assume a plasma composed of deuterium ions in an 8 Tesla magnetic field, the cold plasma dispersion modes are plotted in Figure 7. Here x is the distance along the equatorial plane (with x = 0 being the center of the plasma) and $k_\perp$ is the wavenumber perpendicular to the toroidal magnetic field. The location of the lower hybrid resonance is denoted by LHR. Let us assume a second lower hybrid wave of frequency 2.611 GHz. Then, approximately, v_1 = 40.3 and v_2 = 41.3 (the deuterium cyclotron frequency in the 8 Tesla field being 60.8 MHz). Assuming κ = 1 and ε_1 = ε_2 = 4.9, in Figure 8 we plot the normalized Larmor radius of two ions started with different initial energies ($\rho_0^{(1)}$ = 14.8 and $\rho_0^{(2)}$ = 16.3). The ion started at the higher initial energy makes it into the chaotic region while the ion started at the lower initial energy does not. However, both ions experience nonlinear coherent energization. If the higher frequency wave had a shorter wavelength such that κ = 1.02, then both ions make it into the chaotic regime as shown in Figure 9. Thus, in tokamak plasmas it is possible to energize low-energy ions with two lower hybrid waves whose frequencies differ by the ion-cyclotron frequency. These results can be understood analytically in detail by a second-order perturbation analysis.[25]
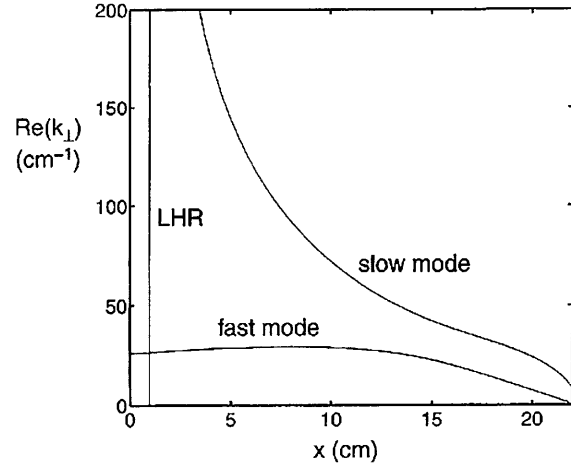

Figure 7. The cold plasma modes for Alcator C-Mod type of parameters. LHR denotes the location of the lower hybrid resonance.
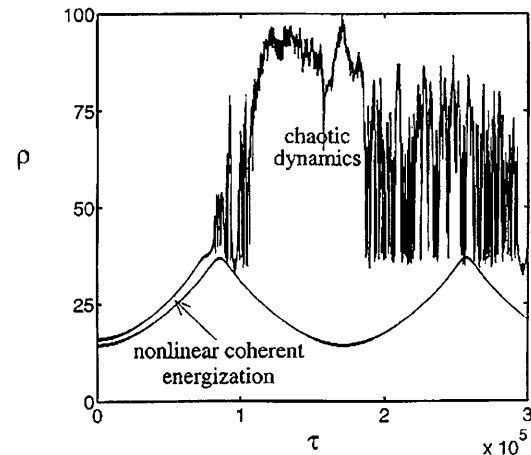

Figure 8. Normalized Larmor radius ρ versus τ for two ions interacting with two waves having the following normalized parameters: ε_1 = ε_2 = 4.9, κ = 1, v_1 = 40.3, and v_2 = 4.13. Initially the ions are started with $\rho_0^{(1)}$ = 14.8, $\psi_0^{(1)}$ = 0, $\rho_0^{(2)}$ = 16.3 and $\psi_0^{(2)}$ = 0.

24 D. Benisti, A.K. Ram, and A. Bers, "New Mechanisms of Ion Energization by Multiple Electrostatic Waves in a Magnetized Plasma," *Phys. Rev. Lett.*, forthcoming; D. Benisti, A.K. Ram, and A. Bers, "Ion Dynamics in Multiple Electrostatic Waves in a Magnetized Plasma. Part I: Coherent Acceleration," submitted to *Phys. Plasmas*; D. Benisti, A.K. Ram, and A. Bers, "Ion Dynamics in Multiple Electrostatic Waves in a Magnetized Plasma. Part II: Enhancement of the Acceleration," submitted to *Phys. Plasmas* ; A.K. Ram, A. Bers, and D. Benisti, "Ionospheric Ion Acceleration by Multiple Electrostatic Waves," *J. Geophys. Res.*, forthcoming.

25 D. Benisti, A.K. Ram, and A. Bers, *Ion Dynamics in Multiple Electrostatic Waves in a Magnetized Plasma*, PSFC/JA-97-22 (Cambridge: MIT Plasma Science and Fusion Center, 1997); D. Benisti, A.K. Ram, and A. Bers, "New Mechanisms of Ion Energization by Multiple Electrostatic Waves in a Magnetized Plasma," *Phys. Rev. Lett.*, forthcoming; D. Benisti, A.K. Ram, and A. Bers, "Ion Dynamics in Multiple Electrostatic Waves in a Magnetized Plasma. Part I: Coherent Acceleration," submitted to *Phys. Plasmas*; A.K. Ram, A. Bers, and D. Benisti, "Ionospheric Ion Acceleration by Multiple Electrostatic Waves," *J. Geophys. Res .*, forthcoming.
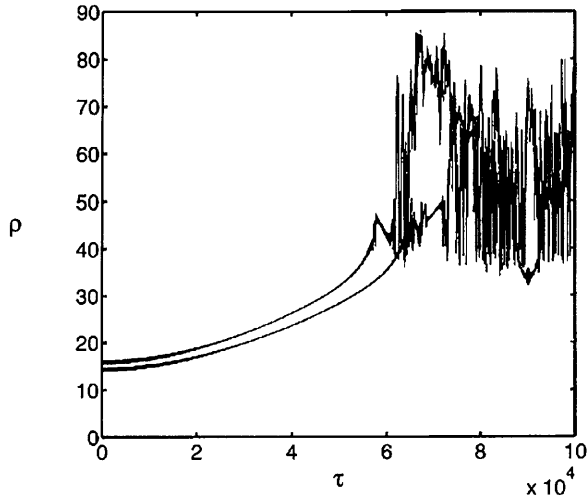
tiple time scale analysis to second order in the amplitudes, we find that an approximate solution of (15) is given by:

$$x(\tau) \approx \rho(\tau)\sin\{\tau + \psi(\tau)\}.$$ (16)

The evolution equations for $\rho(\tau)$ and $\psi(\tau)$ are:

Figure 9. Normalized Larmor radius ρ versus τ for two ions interacting with two waves. The parameters are the same as in Figure 8 except that $\kappa = 1.02$, i.e., the higher frequency wave has the shorter wavelength.

For ions whose energies are below the lower energy bound of the chaotic region [discussed in (12)], we expect that their dynamics can be determined analytically. Toward that end, we carry out a perturbation analysis of (15) using the method of multiple time scales.[26] A more comprehensive and general analytical treatment using the Lie transform perturbation technique has also been developed and is presented elsewhere.[27] The perturbation parameter, in the method of multiple time scales, is the normalized amplitude of the waves. In our analysis we assume that neither v_1 nor v_2 is an integer, i.e., the wave frequencies are not an integer multiple of the ion-cyclotron frequency. However, we will assume that the difference in the frequencies of the two waves is an integer multiple of the ion-cyclotron frequency, i.e., $v_1 - v_2 = N$, an integer. (The analysis can be generalized to the case when $v_1 + v_2 = N$, and also for v_1 and v_2 are integers.[28]) Our analysis breaks down in the vicinity of the chaotic regime. Upon carrying the mul-

$$\frac{\partial\rho}{\partial\tau} = -\frac{\varepsilon_1\varepsilon_2}{2\rho}N\sin(N\psi)\sum_{l=-\infty}^{\infty}\frac{J_l(\rho)J_{l-N}(\kappa\rho)}{1-(l-v_1)^2}$$ (17)

$$\frac{\partial\psi}{\partial\tau} = -\frac{1}{4\rho}\frac{\partial}{\partial\rho}\sum_{l=-\infty}^{\infty}\frac{\varepsilon_1^2J_l^2(\rho)+\varepsilon_2^2J_{l-N}^2(\kappa\rho)}{1-(l-v_1)^2}$$ (18)

$$-\frac{\varepsilon_1\varepsilon_2}{2\rho}\frac{\partial}{\partial\rho}\sum_{l=-\infty}^{\infty}\frac{J_l(\rho)J_{l-N}(\kappa\rho)}{1-(l-v_1)^2}$$

If $\varepsilon_1 = \varepsilon_2 = \varepsilon$, then the above equations become independent of amplitude if we define a new time variable $\bar\tau = \varepsilon^2\tau$. This implies that the change in the Larmor radius of an ion is independent of the amplitude of the two waves. However, the rate at which the Larmor radius changes is inversely proportional to the square of the amplitude. This is an important result. Even if the wave amplitudes are below the threshold for onset of chaotic motion, ions can still get energized. This would not occur in the case of a single wave.

Upon substituting $I = \rho^2/2$, the above evolution equations for the amplitude and the phase can be derived from the Hamiltonian:

$$H(I,\psi) = S_1(I) + \cos(N\psi)S_2(I)$$ (19)

where S_1 and S_2 are the following sums:

$$S_1(I) = \frac{1}{4}\sum_{l=-\infty}^{\infty}\frac{\varepsilon_1^2J_l^2(\rho)+\varepsilon_2^2J_{l-N}^2(\kappa\rho)}{(l-v_1)^2-1}$$ (20)

26   A.H. Nayfeh, *Perturbation Methods* (New York: John Wiley, 1973), pp. 228-307.

27   D. Benisti, A.K. Ram, and A. Bers, *Ion Dynamics in Multiple Electrostatic Waves in a Magnetized Plasma*, PSFC/JA-97-22 (Cambridge: MIT Plasma Science and Fusion Center, 1997); D. Benisti, A.K. Ram and A. Bers, "New Mechanisms of Ion Energization by Multiple Electrostatic Waves in a Magnetized Plasma," *Phys. Rev. Lett.*, forthcoming; D. Benisti, A.K. Ram, and A. Bers, "Ion Dynamics in Multiple Electrostatic Waves in a Magnetized Plasma. Part I: Coherent Acceleration," submitted to *Phys. Plasmas*; D. Benisti, A.K. Ram, and A. Bers, "Ion Dynamics in Multiple Electrostatic Waves in a Magnetized Plasma. Part II: Enhancement of the Acceleration," submitted to *Phys. Plasmas*.

28   D. Benisti, A.K. Ram, and A. Bers, *Ion Dynamics in Multiple Electrostatic Waves in a Magnetized Plasma*, PSFC/JA-97-22 (Cambridge: MIT Plasma Science and Fusion Center, 1997); D. Benisti, A.K. Ram and A. Bers, "Ion Dynamics in Multiple Electrostatic Waves in a Magnetized Plasma. Part I: Coherent Acceleration," submitted to *Phys. Plasmas*.

$$S_2(I) = \frac{1}{2}\varepsilon_1\varepsilon_2 \sum_{l = -\infty}^{\infty} \frac{J_l(\rho)J_{l-N}(\kappa\rho)}{(l-v_1)^2 - 1} \qquad (21)$$

The Hamiltonian equation (19) is independent of time, signifying that it is a new constant, or invariant (to second order in the amplitude), of the dynamics. This constant is determined by the initial conditions $I(\tau = 0)$ and $\overline{\psi}(\tau = 0)$ of an ion. Note that at $\tau = 0$, $\overline{\psi} = \psi$, where ψ is the angle discussed below (10).

If we define $S_1 \pm S_2 = H_\pm$, then

$$H_-(I) = \frac{1}{4} \sum_{l = -\infty}^{\infty} \frac{\{\varepsilon_1 J_l(\rho) - \varepsilon_2 J_{l-N}(\kappa\rho)\}^2}{1 - (l - v_1)^2} \qquad (22)$$

$$H_+(I) = \frac{1}{4} \sum_{l = -\infty}^{\infty} \frac{\{\varepsilon_1 J_l(\rho) + \varepsilon_2 J_{l-N}(\kappa\rho)\}^2}{1 - (l - v_1)^2} \qquad (23)$$

It is easy to note that, algebraically, for $S_2(I) > 0$,

$$H_-(I) \le H(I,\overline{\psi}) \le H_+(I) ; \qquad (24)$$

for $S_2(I) < 0$,

$$H_+(I) \le H(I,\overline{\psi}) \le H_-(I) ; \qquad (25)$$

and for $S_2(I) = 0$,

$$H(I,\overline{\psi}) = H_-(I) = H_+(I) . \qquad (26)$$

Thus the orbits of the ions are bound in energy to lie between two consecutive zeros of $S_2(I)$. The first zero of S_2 occurs at $I = 0$ or, equivalently, at $\rho = 0$. However, this perturbation analysis breaks down as the ions approach the chaotic region which is, approximately, still given by the left-hand side of (12) with $v = \min(v_1, v_2)$.

In Figure 10, we plot a magnified view of H, H_+, and H_- as a function of ρ for the parameters corresponding to Figure 8. The lower bound of the chaotic region is $\rho \approx 30.1$, which is slightly to the right of the bump in H_-. The trajectory of any ion is bound to lie between H_+ and H_- and is given by a straight line parallel to the horizontal axis. Thus any ion started off with initial H below the dashed line will not make it into the chaotic region while ions started off with initial H above the dashed line will. The circle and the cross mark the initial H's of the two ions of Figure 8. It is now clearly evident why the ion which was started off at a slightly higher energy does make it into the chaotic region while the other one does not.
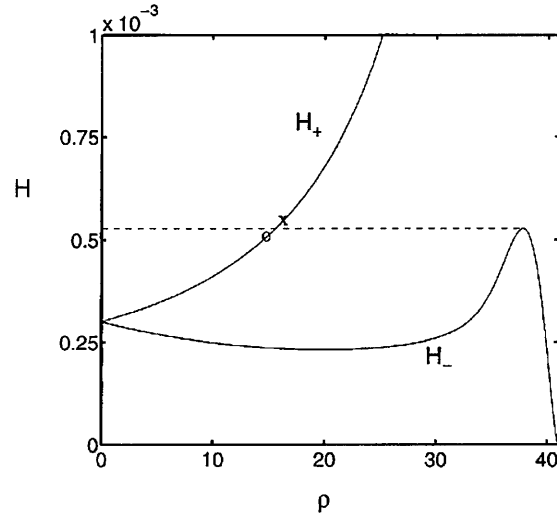

Figure 10. Plot of H_- and H_+ as a function of ρ for parameters corresponding to Figure 8. The dashed line gives the minimum value of H needed to make it into the chaotic region. The circle and the cross mark the initial locations of the two ions of Figure 8.

In Figure 11, we plot a magnified view of H, H_+, and H_- as a function of ρ for the parameters corresponding to Figure 9. Comparing this to Figure 10, we note that the bump in H_- no longer exists. Thus any ion started at a low energy should make it into the chaotic regime. This is in complete agreement with the numerical results displayed in Figure 9. So the second perturbation analysis provides an insight into the nonlinear coherent energization. Furthermore, with an appropriate choice of two lower hybrid waves, it is possible to energize low energy ions in tokamak experiments.
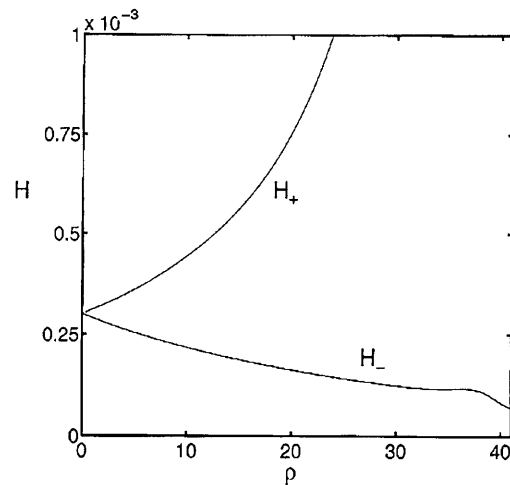

Figure 11. Plot of H_- and H_+ as a function of ρ for parameters corresponding to Figure 9.

1.1.5 Interaction of Bootstrap Current and RF Waves in Tokamaks

Sponsor

U.S. Department of Energy
Grant DE-FG02-91-ER-54109

Project Staff

Steven D. Schultz, Professor Abraham Bers, Dr. Abhay K. Ram

Work is in progress on the interaction of radio frequency (RF) waves and the bootstrap current in tokamaks. By using a Fokker-Planck collisional/quasilinear code, we have performed a kinetic calculation of the electron current in a prescribed density and temperature gradient, for a plasma in the shape of a torus.

The current carried by electrons is found by taking the parallel velocity moment of their distribution function f,

$$J_{\parallel} = -e \int d^3 v \, v_{\parallel} f \quad . \tag{27}$$

We take f to be at steady state, averaged over the gyromotion, and independent of the toroidal angle ϕ by axisymmetry. Under these assumptions, f can be written as a function of the guiding center coordinates r and θ and two constants of the motion, the electron's energy E and magnetic moment μ. Then f satisfies the *drift kinetic equation* (DKE)

$$v_{\parallel} \frac{B_{\theta}}{B} \frac{1}{r} \frac{\partial f}{\partial \theta} + v_{Dr} \frac{\partial f}{\partial r} = C(f) + Q(f) \tag{28}$$

where C(f) is a collision operator, and Q(f) is the quasilinear operator for diffusion due to RF waves.

In *Progress Reports* No. 137 and 138,[29] we described one way of solving (28) through expansion in small parameters. The result was

$$f = f_0^{(o)} + \tilde{f}_1^{(o)} + \hat{f}_1^{(o)} . \tag{29}$$

The modified electron distribution due to RF effects only was the solution to

$$\langle C(f_0^{(o)}) + Q(f_0^{(o)}) \rangle = 0 \tag{30}$$

where the brackets indicate averaging over a bounce orbit. Inclusion of guiding center drifts gives

$$\tilde{f}_1^{(o)} = -\frac{m}{eB_o} v_{\parallel} \frac{\partial f_0^{(o)}}{\partial r} \tag{31}$$

and the additional equation

$$\langle C(\tilde{f}_1^{(o)}) + Q(\tilde{f}_1^{(o)}) \rangle = S \tag{32}$$

with the "source term"

$$S \equiv -\langle C(\tilde{f}_1^{(o)}) + Q(\tilde{f}_1^{(o)}) \rangle . \tag{33}$$

We have been able to reproduce the neoclassical distribution with the Fokker-Planck/neoclassical code FASTFP-NC. This code incorporates the Fokker-Planck code FASTFP,[30] which was created by M. Shoucri and I. Shkarofsky in order to solve the equations (30) and (32). This code is an improvement over those we previously used in that it contains a collision operator with both electron-electron and electron-Maxwellian ion collisions, and that all of the physics are relativistic. The code solves the equation on multiple flux surfaces, assuming a fixed density and background ion temperature, and also includes the particle drifts due to magnetic field gradient and curvature.

We have tested the code by first comparing numerically generated results for Maxwellian plasmas in the low-aspect-ratio limit with the analytically derived results from neoclassical theory.[31] This has been done prior to the inclusion of the RF quasilinear operator. Figure 12 shows a direct comparison of the bootstrap current $J_{\parallel}^{BS}$ for a Maxwellian plasma as calculated by FASTFP-NC and as derived by Rosenbluth, Hazeltine, and Hinton.[32] This shows that it is possible to calculate bootstrap currents kinetically.

29   A. Bers, A.K. Ram, C.C. Chow, V. Fuchs, K.P. Chan, S.D. Schultz, and L. Vacca, "Plasma Wave Interactions—RF Heating and Current Generation," *MIT RLE Progress Report* 137: 229-37 (1994); A. Bers, A.K. Ram, V. Fuchs, J. Theilhaber, F.W. Galicia, S.D. Schultz, and L. Vacca, "Plasma Wave Interactions—RF Heating and Current Generation," *MIT RLE Progress Report* 138: 247-65 (1995).

30   M. Shoucri and I. Shkarofsky, *Comput. Phys. Commun.* 82: 287 (1994); M. Shoucri, I. Shkarofsky, and Y. Peysson, "Numerical Solution of the Fokker-Planck Equation for the Heating and Current Drive Problem," *Centre Canadien de Fusion Magnétique Report* No. CCFM-RI-465e (Varennes, Quebec, Canada: Institut de Recherche de l'Hydro Quebec, 1996); M. Shoucri and I. Shkarofsky, "A Fokker-Planck Code for the Electron-Cyclotron Current Drive and Electron-Cyclotron/Lower Hybrid Current Drive Synergy," *Centre Canadien de Fusion Magnétique Report* No. CCFM-RI-467e (Varennes, Quebec, Canada: Institut de Recherche de l'Hydro Quebec, 1996).

31   M.N. Rosenbluth, R.D. Hazeltine, and F.L. Hinton, *Phys. Fluids* 15: 116 (1972).

The data in Figure 12 and all subsequent runs was made using parameters which fit the physical parameters of a typical high-aspect-ratio tokamak: $R_0 = 2.5$ m, $a = 0.5$ m, $n_e = (10^{20} \text{ m}^{-3}) \times [1 - (r/a)^2]^{0.5}$, $B_T = 4$ T, $1 < q < 3$, and $T_e = T_i = 1$ keV.

The next phase of the analysis involved the use of a quasilinear operator for diffusion in velocity space parallel to the equilibrium magnetic field. Such a diffusion operator can approximate the effects of waves with frequencies smaller than the electron cyclotron frequency, which includes fast Alfvén waves and lower hybrid waves.

A few early runs have been completed which calculate the electron current with parallel diffusion and the bootstrap-generating neoclassical effects. In some cases, this current was found to be slightly larger than the sum of the RF-driven current, and the bootstrap current when each effect is included without the other. Table 1 shows these currents for cases which fit fast wave and lower hybrid current drive scenarios. In the cases shown, there is a small difference in the current calculations taken together and separately. A significant number of future runs will be made to find cases with a more substantial increase in the current.

In future stages of the analysis, first perpendicular diffusion will be included in the quasilinear operator, so that the effects of electron cyclotron waves on the bootstrap current can be calculated. In addition, we will also add to FASTFP-NC the capability to evaluate the RF power deposited on the electrons, and from this a current drive efficiency will be calculated.
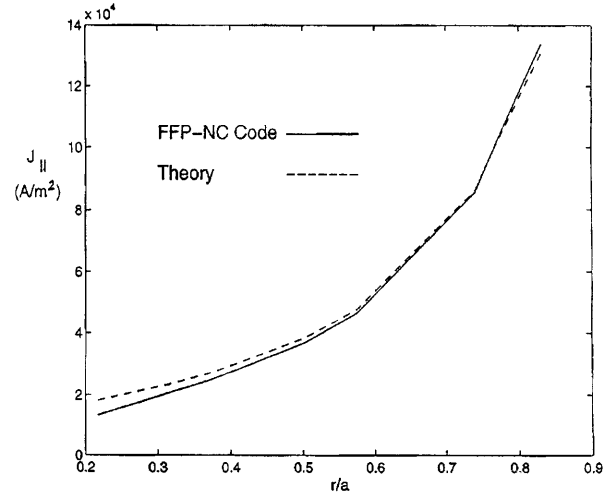

Figure 12. Bootstrap current $J_\parallel^{BS}$ for a Maxwellian plasma from FASTFP-NC (solid line) and Rosenbluth, Hazeltine, and Hinton (dashed line).

Table 2: Electron current $J_\parallel$ from FASTFP-NC which includes neoclassical effects and an RF parallel diffusion coefficient, separately and together.

RF Waves	$D_\parallel/v_c p_t^2$	Range	$J_\parallel$ from FASTEP in MA/m2			
			NC Only	RF Only	Combined	Synergistic
FAW	0.005	$0.5 < \dfrac{v_\parallel}{v_t} < 1.5$	0.31	1.08	1.43	0.04
FAW	0.01	$0.5 < \dfrac{v_\parallel}{v_t} < 1.5$	0.31	1.55	1.90	0.04
LH	0.5	$3.5 < \dfrac{v_\parallel}{v_t} < 8$	0.31	0.10	0.42	0.01

32 M.N. Rosenbluth, R.D. Hazeltine, and F.L. Hinton, *Phys. Fluids* 15: 116 (1972).

1.1.6 Three-Dimensional Space-Time Evolution of Laser-Plasma Instabilities

Project Staff

Ronald J. Focia, Professor Abraham Bers, Dr. Abhay K. Ram

Introduction

We have initiated studies of laser-plasma instabilities relevant to Inertial confinement fusion (ICF). Work carried out in this group some years ago[33] gives the basic approach to determining the space-time evolution of such instabilities in their linear regime.

Instability Analysis

The nonlinearly coupled mode dispersion relations (CMDR) developed by Watson[34] were used to carry out a linear instability analysis of four laser-plasma interactions. The laser-plasma interactions studied here all involve the resonant decay of an incident electromagnetic (EM) wave into two daughter waves in a homogeneous plasma. Resonant decay interactions satisfy the frequency and wavevector matching conditions

$$\omega_L = \omega_1 + \omega_2, \tag{34}$$

and

$$\vec{k}_L = \vec{k}_1 + \vec{k}_2, \tag{35}$$

where ω_L ($\vec{k}_L$) and $\omega_{1,2}$ ($\vec{k}_{1,2}$) are the laser and daughter product frequencies (wavevectors), respectively. In all of the work that follows, the incident laser is assumed to be propagating in the +x-direction and to be plane-polarized in the +z-direction.

The interactions studied are briefly summarized as follows. Stimulated raman scattering (SRS) is the decay into a scattered EM wave and an electron plasma (EP) wave. Stimulated Brillouin scattering (SBS) is the decay into a scattered EM wave and an ion acoustic (IA) wave. The two-plasmon (TP) interaction is the decay into two EP waves. Finally, the plasmon-phonon (PP) interaction is the decay into an EP wave and an IA wave.

The CMDRs for these interactions have the general form

$$D(\vec{k}, \omega) = D_1(\vec{k}, \omega)D_2(\vec{k}, \omega) + \Omega^4, \tag{36}$$

where $D_1(\vec{k},\omega)$ and $D_2(\vec{k},\omega)$ are the uncoupled daughter mode (second order in $\vec{k}$ and ω) dispersion relations and Ω is the nonlinear coupling constant: it depends on the laser field intensity. Neglecting wave damping the CMDRs for the various interactions along with other definitions are summarized in Table 2. Using the matching conditions of (34) and (35) these dispersion relations can be reduced to unknowns in terms of only one wave. Allowing $\vec{k}$ = $\vec{k}_{real}$, the dispersion relation for normal modes, i.e., $D(\vec{k},\omega) = 0$, is solved for $\omega = \omega_r + i\omega_i$. If the imaginary part of ω is greater than zero this indicates growth, i.e. instability. All quantities are first normalized in the following manner. Frequencies are normalized to the laser frequency ω_L, velocities are normalized to the speed of light c, and wavevectors are normalized to ω_L/c. The normalized growthrate for various interactions versus the normalized real k-vector in two dimensions are shown in Figures 13 through 16. In all figures, the growthrate is plotted versus the highest frequency daughter-product wavevector as outlined in Table 2. These plots were generated using an interactive mathematical software tool called MathCad. The shape of the growthrate plots can be explained by considering the geometry effects introduced by the coupling constant Ω and the constraints imposed by (34) and (35).

33 F.W. Chambers, "Space-Time Evolution of Instabilities in Laser-Plasma Interactions," Ph.D. diss., Department of Physics, MIT, 1975; D.C. Watson, "Third Order Theory of Pump-Driven Instabilities—Laser-Pellet Interactions," Ph.D. diss., Department of Electrical Engineering, MIT, 1975; A. Bers, "Linear Waves and Instabilities," in *Plasma Physics* (Les Houches, 1972), (London: Gordon and Breach, 1974); A. Bers, "Space-Time Evolution of Plasma Instabilities-Absolute and Convective," in *Handbook of Plasma Physics,* eds. M.N. Rosenbluth and R.Z. Sagdeev (New York: North-Holland, 1983).

34 D.C. Watson, "Third Order Theory of Pump-Driven Instabilities—Laser-Pellet Interactions," Ph.D. diss., Department of Electrical Engineering, MIT, 1975.

Table 2.

Coupled mode dispersion relations and definition used in the instability analysis.
(Note that subscripts 1 and 2 are used to indicate the uncoupled dispersion functions D_1 and D_2 in (36).)

<u>SRS: EM→EM$_1$+EP$_2$</u>: $D(k, \omega) = (\omega_1^2 - c^2 k_1^2 - \omega_{pe}^2)(\omega_2^2 - 3v_{Te}^2 k_2^2 - \omega_{pe}^2) - \dfrac{v_L^2}{4}\omega_{pe}^2 k_2^2 (\hat{e}_1 \bullet \hat{e}_L)^2$

<u>SBS: EM→EM$_1$+IA$_2$</u>: $D(k, \omega) = (\omega_1^2 - c^2 k_1^2 - \omega_{pe}^2)(\omega_2^2 - c_s^2 k_2^2) - \dfrac{v_L^2 \omega_{pe}^2 c_s^2}{4 v_{Te}^2}k_2^2 (\hat{e}_1 \bullet \hat{e}_L)^2$

<u>TP: EM→EP$_1$+EP$_2$</u>: $D(k, \omega) = (\omega_1^2 - 3v_{Te}^2 k_1^2 - \omega_{pe}^2)(\omega_2^2 - 3v_{Te}^2 k_2^2 - \omega_{pe}^2) - \dfrac{v_L^2}{4}[(\hat{e}_1 \bullet \hat{e}_L)\omega_1 k_2 + (\hat{e}_2 \bullet \hat{e}_L)\omega_2 k_1]^2$

<u>PP: EM→EP$_1$+IA$_2$</u>: $D(k, \omega) = (\omega_1^2 - 3v_{Te}^2 k_1^2 - \omega_{pe}^2)(\omega_2^2 - c_s^2 k_2^2) - \dfrac{v_L^2}{4v_{Te}^2}\omega_1^2 \omega_2^2 (\hat{e}_1 \bullet \hat{e}_L)^2$

<u>Electron quiver velocity due to the laser electron field</u>: $v_L = \left|\dfrac{eE_L}{m_e \omega_L}\right|$

<u>Electron thermal velocity</u>: $v_{Te} = \left(\dfrac{k_B T_e}{m_e}\right)^{1/2}$ <u>Ion acoustic speed</u>: $c_s = \left[\dfrac{3k_B T_i}{M_i} + \dfrac{k_B T_e}{M_i}\right]^{1/2}$

$\hat{e}_i$ is the polarization vector for mode i.

$$
\begin{array}{ll}
P_L = & 10^{16}\ \text{W/cm}^2 \\
\lambda_L = & 526.5\ \text{nm} \\
T_e = & 1\ \text{keV} \\
T_i = & 50\ \text{eV} \\
\omega_{pe}/\omega_L = & \sqrt{\dfrac{n}{n_{crit}}} = 0.45 \\
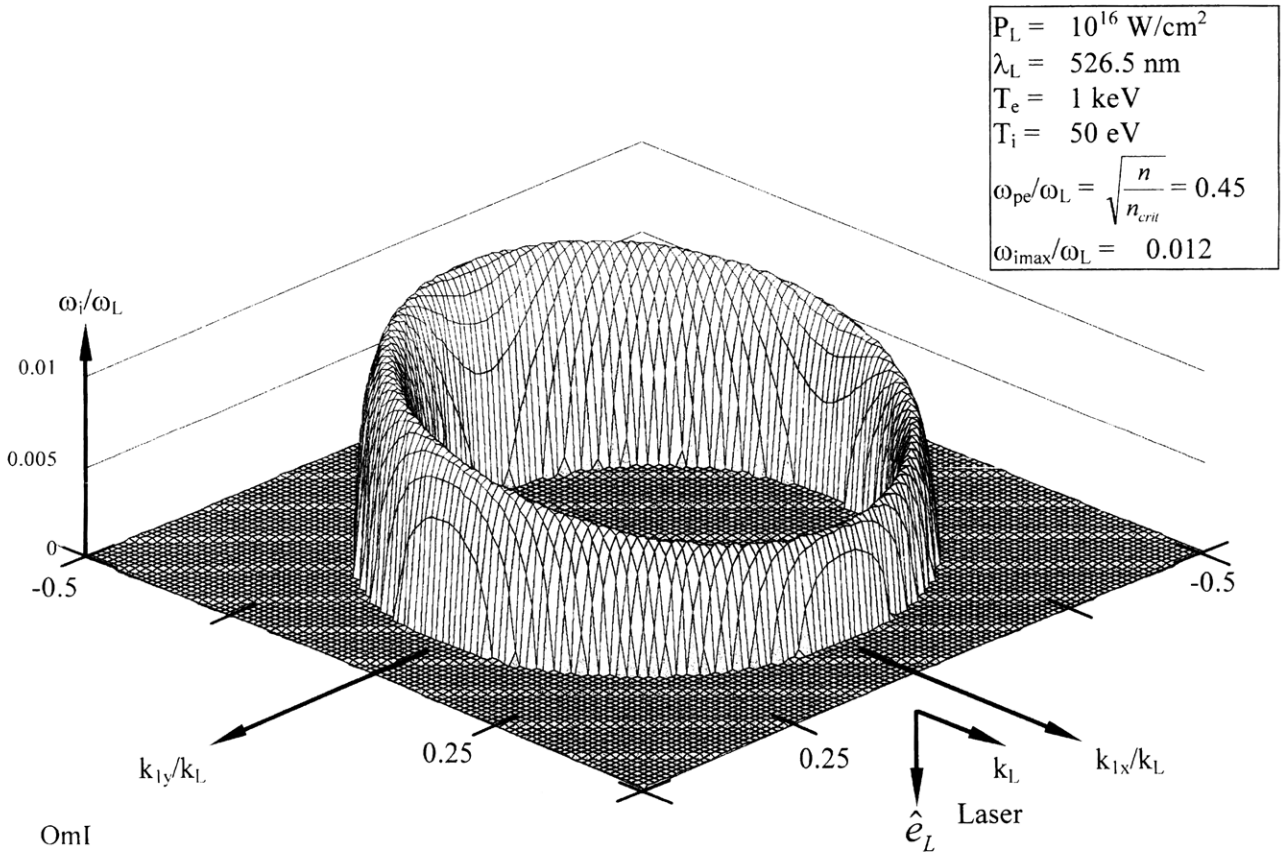\omega_{imax}/\omega_L = & 0.012
\end{array}
$$

Figure 13. Normalized growthrate, $\omega_i(k_r)/\omega_L$, for the stimulated raman scattering (SRS) interaction plotted in the k_{1x}-k_{1y} plane. The scattered EM wave is assumed to be polarized in the z direction.
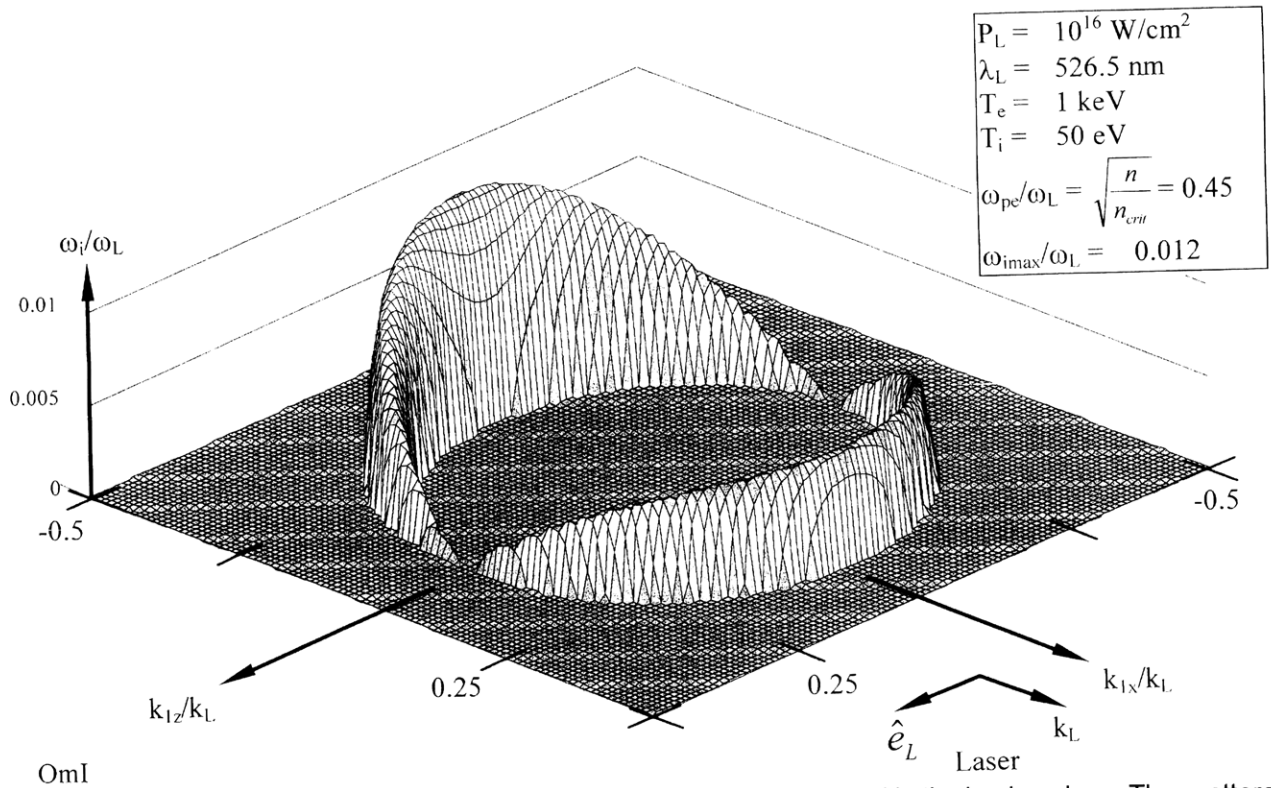
Figure 14. Normalized growthrate, $\omega_i(k_r)/\omega_L$, for the SRS interaction plotted in the k_{1x}-k_{1z} plane. The scattered EM wave is assumed to be polarized in the x-z plane.
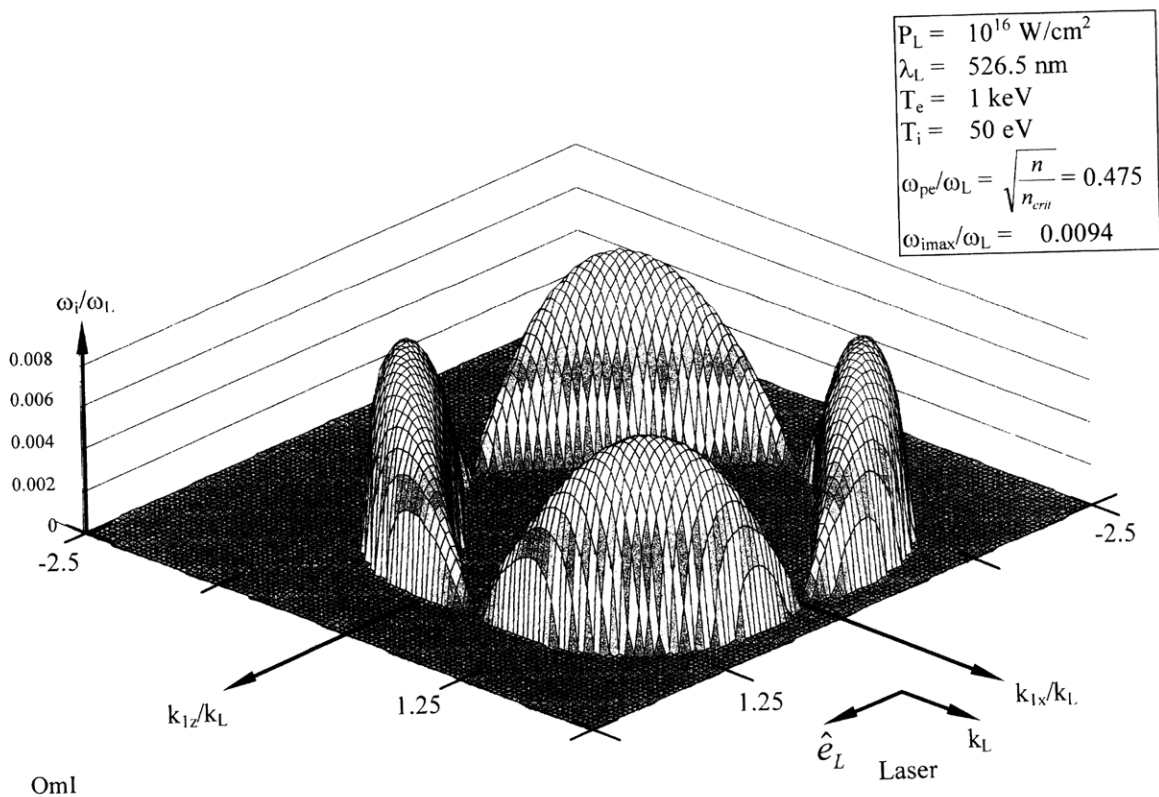

Figure 15. Normalized growthrate, $\omega_i(k_r)/\omega_L$, for the TP interaction plotted in the k_{1x}-k_{1z} plane.
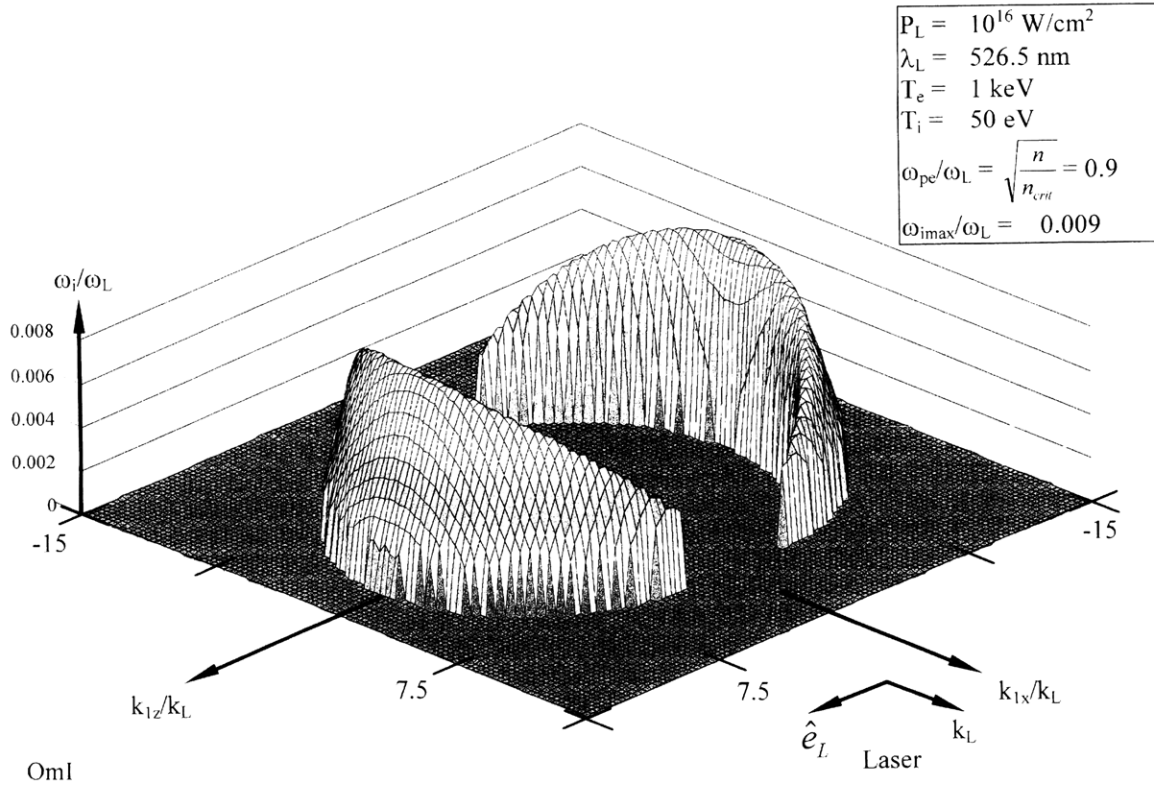
$P_L =$	10^{16} W/cm^2
$\lambda_L =$	526.5 nm
$T_e =$	1 keV
$T_i =$	50 eV
$\omega_{pe}/\omega_L = \sqrt{\dfrac{n}{n_{crit}}} = 0.9$	
$\omega_{imax}/\omega_L =$	0.009

Figure 16. Normalized growthrate, $\omega_i(k_r)/\omega_L$, for the PP interaction plotted in the k_{1x}-k_{1z} plane.

Asymptotic Pulse Response in Three Dimensions

The time asymptotic impulse response, or Green's Function, of each interaction was also evaluated using the Bers-Briggs pinch point analysis.[35] In this method, the time asymptotic response is calculated for an observer moving at a velocity $\vec{V} = \vec{r}/t$ and the spatial response is determined by considering all possible $\vec{V}$. Expanding the CMDR about any $(\vec{k} = \vec{k}_0, \omega = \omega_0)$ that satisfy (34) and (35) results in the Two-Wave Coupling Dispersion Relation (TWCDR)

$$D(k, \omega) = [(\omega - \omega_0) - \vec{v}_1 \bullet (\vec{k} - \vec{k}_0) + i\nu_1] \quad , \quad (37)$$
$$[(\omega - \omega_0) - \vec{v}_2 \bullet (\vec{k} - \vec{k}_0) + i\nu_2] + \gamma^2$$

where $\vec{v}_1$ and $\vec{v}_2$ are the wave group velocities, ν_1, ν_2 are weak damping rates of the daughter waves at $(\vec{k}_0, \omega_0)$, and $\gamma^2 = \dfrac{\Omega^4}{\left.\dfrac{\partial D_1}{\partial \omega}\right|_{\omega_1} \left.\dfrac{\partial D_2}{\partial \omega}\right|_{\omega_2}}$. The space-time asymptotic evolution of the instability is given by the time asymptotic Green's function $G(\vec{r}, t)$ for an observer moving with velocity $\vec{V}$ relative to the frame in which the dispersion relation is of interest. One thus finds, for nonrelativistic $\vec{V}$'s,[36]

$$\ln\left|G(\vec{r}, t \to \infty)\right| = \gamma_p(\vec{V})t \qquad (38)$$

---

35 A. Bers, "Linear Waves and Instabilities," in *Plasma Physics* (Les Houches, 1972), (London: Gordon and Breach, 1974); A. Bers, "Space-Time Evolution of Plasma Instabilities-Absolute and Convective," in *Handbook of Plasma Physics*, eds. M.N. Rosenbluth and R.Z. Sagdeev, (New York: North-Holland, 1983); R.J. Briggs, *Electron Stream Interaction with Plasmas* (Cambridge, Massachusetts: MIT Press, (1964).

36 A. Bers, "Space-Time Evolution of Plasma Instabilities-Absolute and Convective," in *Handbook of Plasma Physics* , eds. M.N. Rosenbluth and R.Z. Sagdeev, (New York: North-Holland, 1983).

The pinch point growthrate $\gamma_p(\vec{V})$ is determined from the imaginary part of ω which simultaneously satisfies

$$D(\omega + \vec{k} \cdot \vec{V}, \vec{k}) = 0, \tag{39}$$

and

$$\frac{\partial D(\omega + \vec{k} \cdot \vec{V}, \vec{k})}{\partial \vec{k}} = 0 \tag{40}$$

Applying (39) and (40) to (37), it can be shown that a necessary condition is $(\vec{V} - \vec{v_1}) \| (\vec{V} - \vec{v_2})$. The three-dimensional problem is reduced to calculating a set of equivalent one-dimensional absolute instability evolutions for which the pinch point growthrate is given by[37]

$$\gamma_p(V_\|) = \frac{2\gamma}{V_1 + V_2}\sqrt{(V_1 - V_\|)(V_\| + V_2)}$$
$$- \frac{[v_1(V_\| + V_2) + v_2(V_1 - V_\|)]}{V_1 + V_2} \tag{41}$$

The definitions and constructions of $V_\|$, V_1, and V_2 are given in Figure 17. Once again, MathCad was used to create interactive worksheets to generate the pulse shape plots for the SRS and SBS interactions shown in Figure 18 and Figure 19. Inputs to the worksheet are the laser intensity and wavelength, the electron and ion temperatures, and the electron density. For the cases shown we have taken $v_1 = 0 = v_2$. The input variables for the particular plot are given in part (a) of each figure. The asymptotic space-time evolution of the instability is self-similar and hence found by multiplying the observer velocities by time to give the spatial positions, and the pinch point growth rate by time as in (38) to obtain the logarithmic magnitude of the time-asymptotic Green's function. Since the data is actually four-dimensional (4D) visualization is difficult and for now has been reduced to three dimensions by looking at specific planes in the observer velocity space.

Future work will incorporate phenomenological mode damping and relativistic corrections into the expression for the time asymptotic growthrate, as well as other cuts of the 4D evolution.
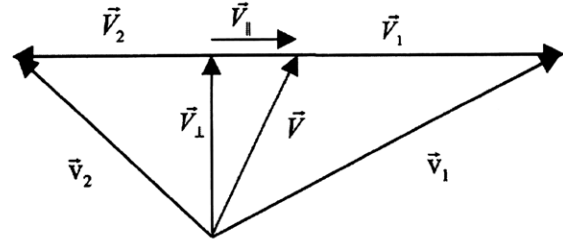
Figure 17. Definitions and constructions of velocity vectors in 3-D Green's function evaluation.

Figure 18. (a) Pulse shape and (b) contour plot for the SRS pinch point growthrate plotted in the V_x-V_y plane. Note that numerical values in x and y are to be multiplied by ct and amplitudes on vertical axis by t. In (b), the outermost contour is zero, the maximum is marked with an "**x**," and each contour represents a 10% change.

---

37 A. Bers, "Linear Waves and Instabilities," in *Plasma Physics* (Les Houches, 1972), (London: Gordon and Breach, 1974).

(a)

(b)

Figure 19. (a) Pulse shape and (b) contour plot for the SBS pinch point growthrate plotted in the V_x-V_y plane. Note that numerical values in x and y are to be multiplied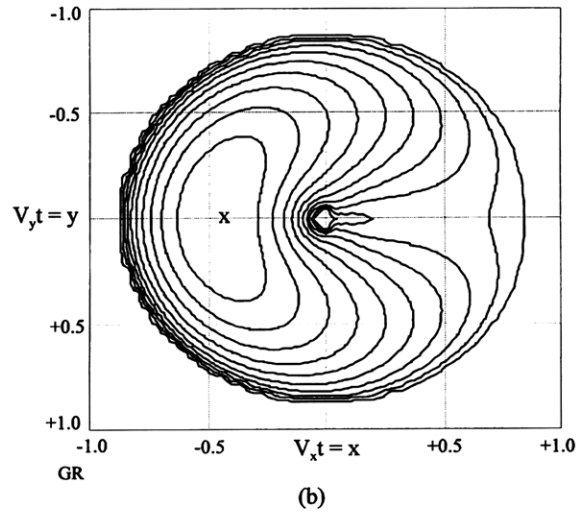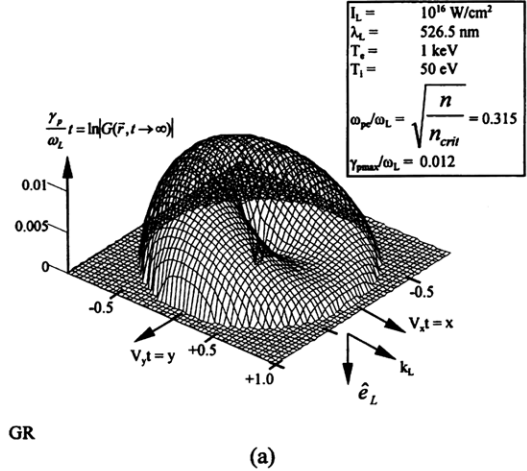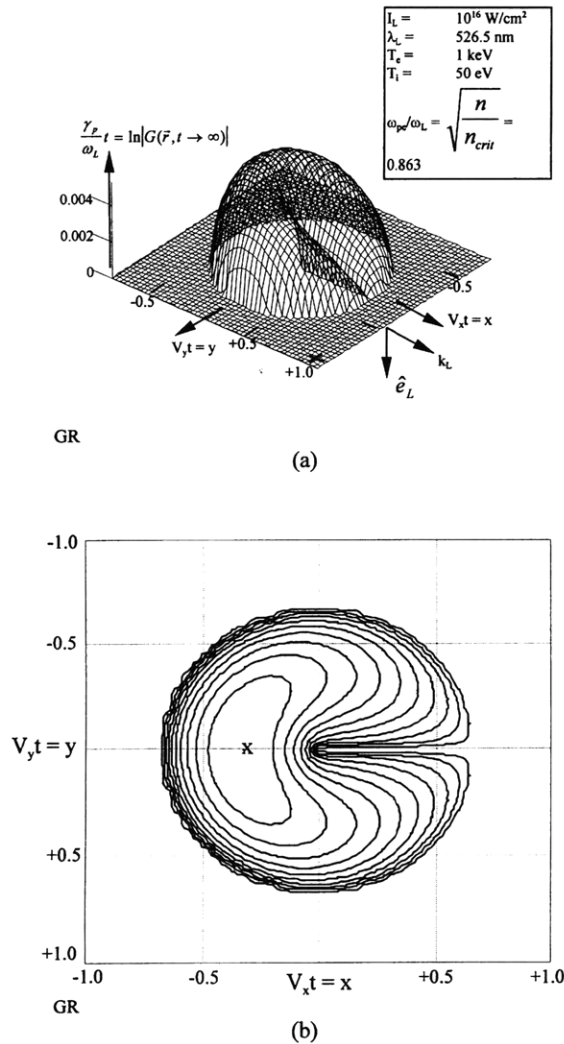 by ct and amplitudes on vertical axis by t. In (b), the outermost contour is zero, the maximum is marked with an "**x**," and each contour represents a 10% change.

1.1.7 Publications

Journal Articles

Benisti, D., A.K. Ram, and A. Bers. "Ion Dynamics in Multiple Electrostatic Waves in a Magnetized Plasma. Part I: Coherent Acceleration." Submitted to *Phys. Plasmas*.

Benisti, D., A.K. Ram, and A. Bers. "Ion Dynamics in Multiple Electrostatic Waves in a Magnetized Plasma. Part II: Enhancement of the Acceleration." Submitted to *Phys. Plasmas*.

Benisti, D., A.K. Ram, and A. Bers. "Lower Bound in Energy for Chaotic Dynamics of Ions." *Phys. Lett. A.* 233: 209 (1997).

Benisti, D., A.K. Ram, and A. Bers. "New Mechanisms of Ion Energization by Multiple Electrostatic Waves in a Magnetized Plasma." Submitted to *Phys. Rev. Lett.*

Bers, A., A.K. Ram, and D. Benisti. "Transverse Acceleration of Ions by Electrostatic Waves in the Earth's Ionosphere." *Bull. Am. Phys. Soc.* 42: 1889 (1997).

Jergovic, I., S.D. Schultz, A.K. Ram, A. Bers and K.C. Wu. "Heating by Electron Cyclotron Waves in NSTX." *Bull. Am. Phys. Soc.* 42: 1934 (1997).

Lashmore-Davies, C.N., V. Fuchs, A.K. Ram, and A. Bers. "Enhanced Coupling of the Fast Wave to Electrons through Mode Conversion to the Ion Hybrid Wave." *Phys. Plasmas* 4: 2031 (1997).

Ram, A.K., D. Benisti, and A. Bers. "Nonlinear Coherent Energization of Ions in Two Electrostatic Waves." *Bull. Am. Phys. Soc.* 42: 2036 (1997).

Ram, A.K., A. Bers, and D. Benisti. "Ion Energization in the Ionosphere by Wave-Particle Interactions." *Eos* (American Geophysical Union Fall Meeting supplement) 78: F613 (1997).

Ram, A.K., D. Benisti, and A. Bers, "Ionospheric Ion Acceleration by Multiple Electrostatic Waves." *J. Geophys. Res.* Forthcoming.

Schultz, S.D., A. Bers, and A.K. Ram. "Effects of RF Waves on the Bootstrap Current in Tokamaks." *Bull. Am. Phys. Soc.* 42: 1930 (1997).

Conference Papers

Ram, A.K. and A. Bers. "Efficient Current Drive by Mode-Converted Ion-Bernstein Waves." *Proceedings of the 12th Topical Conference on Radio Frequency Power in Plasmas*, Savannah, Georgia, April 1-3, 1997. Eds. P.M. Ryan and T. Intrator. Woodbury, New York: AIP Conference Proceedings 403, 1997, pp. 277-80.

Ram, A.K., D. Benisti, and A. Bers. "Ion Acceleration in Multiple Electrostatic Waves." *Proceedings of the Fourth IPELS Conference*, Maui, Hawaii, June 23-27, 1997, p. 25.

Ram, A.K., D. Benisti, and A. Bers, "Nonlinear Coherent Energization of Magnetized Ions in Two or More Electrostatic Waves." *Proceedings of the International Sherwood Fusion Theory Conference*, Madison, Wisconsin, April 28-30, 1997, Paper 1D38.

Schultz, S.D., A. Bers, and A.K. Ram. "Mode-Conversion to Ion-Bernstein Waves of Fast Alfvén Waves With Poloidal Wavenumbers in Sheared Magnetic Fields." *Proceedings of the 12th Topical Conference on Radio Frequency Power in Plasmas*, Savannah, Georgia, April 1-3, 1997. Eds. P.M. Ryan and T. Intrator. *AIP Conference Proceedings* 403, 1997, pp. 331-34.

Schultz, S.D., A. Bers, and A.K. Ram. "RF Effects on Neoclassical Theory and the Bootstrap Current in Tokamaks." *Proceedings of the 12th Topical Conference on Radio Frequency Power in Plasmas*, Savannah, Georgia, April 1-3, 1997. Eds. P.M. Ryan and T. Intrator. Woodbury, New York: AIP Conference Proceedings 403, 1997, pp. 327-30.

Schultz, S.D., A. Bers, and A.K. Ram. "RF Effects on Neoclassical Theory and the Bootstrap Current in Tokamaks." *Proceedings of the International Sherwood Fusion Theory Conference*, Madison, Wisconsin, April 28-30, 1997, Paper 1C30.

Wu, K.C., A.K. Ram, A. Bers, and S.D. Schultz. "Electron Cyclotron Heating in NSTX." *Proceedings of the 12th Topical Conference on Radio Frequency Power in Plasmas*, Savannah, Georgia, April 1-3, 1997. Eds. P.M. Ryan and T. Intrator. Woodbury, New York: AIP Conference Proceedings 403, 1997, pp. 207-10.

Technical Reports

Benisti, D., A.K. Ram, and A. Bers. "Ion Dynamics in Multiple Electrostatic Waves in a Magnetized Plasma." PSFC/JA-97-22. Cambridge: MIT Plasma Science and Fusion Center, October 1997.

Benisti, D., A.K. Ram, and A. Bers. "Lower Bound in Energy for Chaotic Dynamics of Ions." PSFC/JA-97-06. Cambridge: MIT Plasma Science and Fusion Center, April 1997.

Ram, A.K., and A. Bers. *Efficient Current Drive by Mode-Converted Ion-Bernstein Waves.* PSFC/JA-97-07. Cambridge: MIT Plasma Science and Fusion Center, April 1997.

Ram, A.K., D. Benisti, and A. Bers. "Ionospheric Ion Acceleration by Multiple Electrostatic Waves." PSFC/JA-97-19. Cambridge: MIT Plasma Science and Fusion Center, September 1997.

Schultz, S.D., A. Bers, and A.K. Ram. "Mode-Conversion to Ion-Bernstein Waves of Fast Alfvén Waves With Poloidal Wavenumbers in Sheared Magnetic Fields." PSFC/JA-97-08. Cambridge:

MIT Plasma Science and Fusion Center, April 1997.

Schultz, S.D., A. Bers, and A.K. Ram. "RF Effects on Neoclassical Theory and the Bootstrap Current in Tokamaks." PSFC/JA-97-09. Cambridge: MIT Plasma Science and Fusion Center, April 1997.

Wu, K.C., A.K. Ram, A. Bers, and S.D. Schultz. "Electron Cyclotron Heating in NSTX." PSFC/JA-97-10. Cambridge: MIT Plasma Science and Fusion Center, April 1997.

Thesis

Wu, K.C. *Mode Conversion of Electron Cyclotron Waves to Electron Bernstein Waves.* M.Eng. thesis, Department of Electrical Engineering and Computer Science, MIT, May 1997.

1.2 Physics of Thermonuclear Plasmas

Sponsor

Project Staff

Professor Bruno Coppi, Dr. Augusta Airoldi, Vitali Belevtsev, Dr. Madhurjya Bora, Dr. Giuseppe Bertin, Dr. Francesca Bombarda, Franco Carpignano, Dr. Giovanna Cenacchi, Dr. William S. Daughton, Darin R. Ernst, G. Felice, Ming-Hui Kuang, Dmitri Laveder, Dr. Riccardo Maggiora, Dr. Stefano Migliuolo, Peter P. Ouyang, Dr. Francesco Pegoraro, Gregory E. Penn, Evan H. Reich, Marco Riccitelli, Caterina Riconda, Dr. Linda E. Sugiyama, George M. Svolos, Dr. Motohiko Tanaka

1.2.1 Introduction

This research program has, for its primary activity, the theoretical study of magnetically confined plasmas in regimes of relevance to present day advanced experiments, as well as the proposal and planning of new experiments directed towards the study of fusion burning plasmas. The U.S. fusion program has been recently redirected from its emphasis on attempting to develop a viable power producing reactor on the basis of existing knowledge to one supporting basic science and innovative concepts. Our group, with its long term research program on the fundamental physics and its implications for ignition, is directly in line with the new goals of this program.

Our group has been the first to undertake the proposal and the study of magnetically confined ignition experiments, taking a leading role in the development of both their physics and their engineering. The Ignitor experiment (Figure 20) was the first proposed (originally in 1975), designed on the basis of the known physics of thermonuclear plasmas and presently available technology, in order to reach ignition regimes. This year, the construction of the full size protoypes of the main components of this machine has been completed. Our group has always recognized the importance of ignition and devoted attention to it even when its relevance was not universally acknowledged.
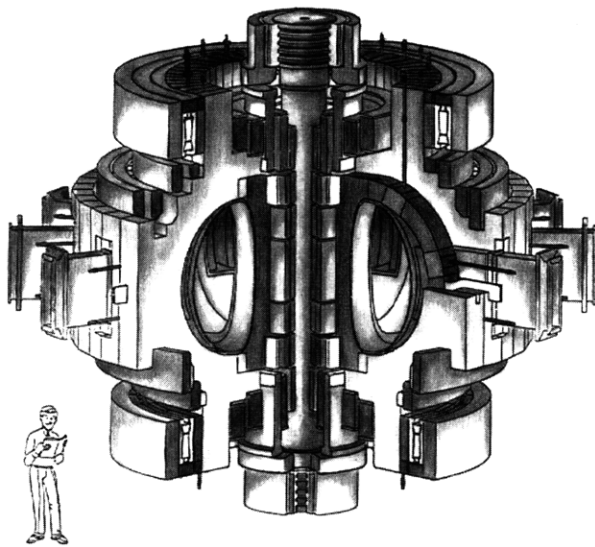

Figure 20.   Ignitor Ult machine.

The importance of providing an experimental proof of the process of ignition has recently been reaffirmed by a high level DOE panel, and we recall the statement[38] by the Panel on Fusion Research of the President's Committee of Advisors on Science and Technology (PCAST): "Producing an ignited plasma will be a truly notable achievement for mankind and will capture the public's imagination. Resembling a burning star, the ignited plasma will demonstrate a capability with immense potential to improve human well-being. Ignition is analogous to the first airplane flight or the first vacuum-tube computer."

It has become increasingly clear that the most suitable and cost effective type of experiment to pursue the goal of ignition is the line of machines that operate at high magnetic field, employing cryogenic normal conducting magnets, which we have pioneered. These are represented by the series of Alcator machines at MIT and the FT machines at Frascati, Italy, and by the Ignitor experiment, which is specifically intended to study ignition conditions. In fact, the ITER design of a large volume D-T burning machine that has been proposed more recently has been evolving toward engineering design solutions and a physics ignition path similar to the one developed for Ignitor. This involves limiting as far as possible the reliance on injected heating, controlling the evolution of the current density profile for reasons of plasma stability, and adopting a similar confinement configuration with the same low aspect ratio and similar structural solutions for the relevant magnet systems. Furthermore, during its design process the limitations of a large scale experiment based on existing superconducting magnet technologies have become more evident. In fact, our view that the technology needed for power-producing fusion reactors should be developed in parallel with but separately from the experiments that are needed to investigate physical regimes relevant to fusion burn conditions has now become widely accepted around the world.

At MIT, the Alcator C-Mod experiment, combining the favorable features of an elongated plasma cross section with a high magnetic field to produce high plasma currents and contain high plasma densities, is being successfully operated and has again demonstrated the intrinsic ability of high field, compact devices to span a wide range of plasma parameters. This machine has characteristics very similar to a proposed experiment called Megator, which we studied in the early seventies as a logical evolutio of the Alcator program we had just established at MIT. Megator was intended to produce multi-megampere plasma currents by combining high magnetic fields, tight aspect ratios and elongated plasma cross sections.

Our group has maintained a pioneering role in the physics of high temperature plasmas, contributing original ideas that have been later taken up by others. Of note are the region of second stability for finite pressure plasmas and the method of raising the central q_0 well above unity to access it, the principle

---

38   Report to the Fusion Review Panel, President's Committee of Advisors on Science and Technology, O.S.T.P., White House, Washington, D.C. (1995).

of profile consistency of the electron temperature, the degradation of energy confinement by ion temperature gradient driven modes, the isotopic effect, the existence of impurity-driven modes localized at the plasma edge, the stabilization of sawteeth by energetic particles, and the time dependent path to ignition in magnetically confined plasmas.

The ideas concerning transport processes in high temperature plasmas and the fact that they can be nonlocal in nature, as indicated for example by the principle of profile (temperature) consistency that we put forward originally, have been confirmed by different experiments carried out around the world and form the basis of several widely adopted approaches to the theory of plasma transport.

The theoretical transport model that we have proposed, involving the excitation of the so-called ITG modes (toroidal ion temperature gradient driven modes that we had found in 1974) and that of collisionless trapped electron modes (that we had also found originally in 1973), has encountered wide acceptance and is incorporated in several sophisticated codes that have been used successfully to interpret present experiments and are attracting widespread interest.

We recall that the suggestion that we had made in the eighties to produce peaked plasma density profiles in the Alcator C experiment, in order to avoid the confinement degradation that was afflicting it, originated from the idea that the excitation of ITG modes was the likely cause. The success of the pellet injection experiments, with the purpose of producing peaked density profiles that were later carried out and led to record values of the confinement parameter $n\tau$ in Alcator, supported the validity of the relevant transport model. We also notice that the enhanced confinement regimes which have been discovered more recently, e.g., by producing a negative magnetic shear configuration, involve the triggering of a state characterized by peaked density profile.[39]

The so-called "isotopic effect" on plasma confinement, where confinement is observed to improve with heavier isotopes of hydrogen, of which we were the first to point out the importance[40] and for which

we provided the first theoretical model,[41] has continued to attract strong interest. Consistent with our expectations, it has been found to be present also in the transport of angular momentum in rotating plasmas.

The first suggestion to use a divertor to improve the energy confinement was included in a paper by Coppi, Rosenbluth and Sagdeev in 1976, as a result of the analysis of the properties of the elementary η_i-modes driven by the ion temperature gradient that can be found in a one-dimensional geometry. The same analysis was used as the basis for introducing an effective diffusion coefficient of the thermal energy that has become popular in recent years and is commonly referred to as the "gyro-Bohm" coefficient.

There is an increasing body of experimental evidence supporting the elements that characterize the so-called second stability region for finite β plasmas, that we had discovered originally, such as the good confinement characteristics of regimes with vanishing magnetic shear. We have followed closely these developments and those concerning experiments with reversed shear, given their intrinsic value, but also in view of the fact that these regimes can be explored in ignited plasmas by experiments of the Ignitor type.

Internal modes that can locally destroy the magnetic field configuration, for which we developed the original theory and analyses, have been recognized by the international community as important potential obstacles to reaching ignition conditions. This is a particularly serious issue for the stated objectives of the ITER project, given the choice of its parameters dictated by the adoption of superconducting magnets.

The series of experiments with deuterium-tritium plasmas that have been carried out recently has renewed our interest in a series of problems related to the presence of energetic particle populations in magnetically confined, thermal plasmas. Among these we point out that the radiation emission at the harmonics of the ion cyclotron frequency of the fusion products in D-T plasmas finds a consistent explanation[42] in the theory of spatially localized

39 F.M. Levington, M.C. Zarnstorff, S.H. Batha, et al., *Phys. Rev. Lett.* 75: 4417 (1995).

40 B. Coppi, G. Lampis, F. Pegoraro, L. Pieroni, and S. Segre, MIT Report PRR - 75/24 (1975).

41 B. Coppi, *Plasma Physics and Controlled Nuclear Fusion 1990*, 2: 413 (Vienna, Austria: International Atomic Energy Agency, 1991).

42 B. Coppi, *Phys. Lett. A* 172: 439 (1993).

modes, that was developed originally by us for spin polarized fusion plasmas.[43] The validity of this analysis has been widely verified by now, and we are pursuing it farther in view of its potential applications, such as to infer easily the radial distribution of the α-particle population from the spectrum of the relevant emitted radiation, in future D-T burning plasma experiments.

Referring to subjects, in the same general area, that have received renewed interest recently, we mention that an extensive paper concerning the effects of α-particles on ballooning and shear-Alfvén modes was published in 1981 in *Annals of Physics* by Coppi and Pegoraro.

We have developed and continue to have a strong interest in studying experiments that can be designed on the basis of present day technologies and can investigate the fusion burning conditions of tritium-poor, nearly pure deuterium plasmas or deuterium-helium 3 plasmas. These experiments are based on combining the main characteristics of high field machines (e.g., Ignitor) with the physics of burning plasmas whose hot core enters the second stability region.

Our analyses of the properties of the plasmas produced by the Alcator C-Mod device has led us to identify salient characteristics of the physical regimes that have been accessed, which give valuable theoretical insights into the nature of the relevant energy transport processes and are expected to be important for future experiments.

1.2.2 The Ignitor Experiment

We have pursued a consistently long term project on the design and physics of tight aspect ratio, high magnetic field experiments that are intended to investigate D-T fusion ignition conditions using presently available technology. Our studies have shown that the most promising and advantageous ignition designs should rely on an interlocking set of characteristics[44]—tight aspect ratio, relatively small size with significant vertical elongation, high toroidal and poloidal magnetic fields, large plasma currents, high plasma densities, good plasma purity, strong ohmic heating, good plasma and α-particle confinement, and robust stability against ideal MHD and resistive plasma instabilities. These criteria have formed the basis for our design of the Ignitor Ult[45] experiment. We note that the ITER design has been evolving, independently, in a similar direction.

Work on the design and construction of one complete sector (1/12th) of the Ignitor-Ult machine has been progressing in Italy. Results of the in-depth analysis of the machine have been reported to the last meeting of the Division of Plasma Physics of the American Physical Society.

As a measure of the momentum of the Ignitor project, the last four meetings of the Division of Plasma Physics of the American Physical Society (1994-97) have each had a sub-session devoted to Ignitor. In the last two years, a total of 15 presentations were given.[46] The titles give some idea of the scope of the work being carried out by the Ignitor design team.

43 B. Coppi, S. Cowley, P. Detragiache, R. Kulsrud, and F. Pegoraro, *Phys. Fluids* 29: 4060 (1986).

44 B. Coppi, M. Nassi, and L.E. Sugiyama, "Physics Basis for Compact Ignition Experiments," *Phys. Scripta* 45: 112-32 (1992)

45 B. Coppi, M. Nassi, and L.E. Sugiyama, "Physics Basis for Compact Ignition Experiments," *Phys. Scripta* 45: 112-32 (1992); B. Coppi and the Ignitor Project Group, *J. Fusion Energy* 13: 111 (1994).

46 The Ignitor Project Group, and B. Coppi, "Present Context of Fusion Research and the Ignitor Experiment," *Bull. Am. Phys. Soc.* 41(10): 1488 (1996); G. Cennachi, A. Airoldi, F. Bombarda, B. Coppi, and J.A. Snipes, "Assessment of Recent Results on Transport and Expectations for Ignitor," *Bull. Am. Phys. Soc.* 41(10): 1488 (1996); A. Airoldi, G. Cenacchi, and B. Coppi, "Ignition Approach Under L-mode Scaling in Ignitor," *Bull. Am. Phys. Soc.* 41(10): 1488 (1996); M. Roccella, G. Cenacchi, M. Gasparotto, C. Rita, A. Pizzuto, B. Coppi, and L. Lanzavecchia, "Plasma Engineering in the Ignitor Experiment," *Bull. Am. Phys. Soc.* 41(10): 1488 (1996); A. Pizzuto, A. Capriccioli, M. Gasparotto, A. Palmieri, C. Rita, M. Roccella, and B. Coppi, "Radial Electromagnetic Press for Ignitor," *Bull. Am. Phys. Soc.* 41(10): 1488 (1996); C. Ferro and F. Bombarda, "First Wall in the Ignitor Machine," *Bull. Am. Phys. Soc.* 41(10): 1489 (1996); M. Riccitelli, B. Coppi, C.K. Phillips, R.P. Majeski, J.R. Wilson, D.N. Smithe, and G. Vecchi, "ICRF Heating Scenarios for the Ignitor Machine," *Bull. Am. Phys. Soc.* 41(10): 1489 (1996); R. Maggiora, G. Vecchi, M. Riccitelli, and M.D. Carter, "Electrical Design of an ICRF System for Ignitor," *Bull. Am. Phys. Soc.* 41(10): 1489 (1996); M.H. Kuang and L.E. Sugiyama, "Reversed Shear Ignition Regimes for High Field Tokamaks," *Bull. Am. Phys. Soc.* 41(10): 1489 (1996); A. Airoldi, G. Cenacchi, B. Coppi, "Fusion Performance of High Magnetic Field Experiments," *Bull. Am. Phys. Soc.* 41(10): 1834 (1997); G. Galas-So, L. Lanzavecchia, G. Dalmut, G. Dra-Go, A. Laurenti, R. Marabotto, G. Ghia, G. Munaro, M. Pirozzi, L. Destefanis, R. Andreani, C. Crescenzi, A. Cucchiaro, M. Gasparotto, A. Pizzuto, and B. Coppi, "Ignitor Prototype Construction Program," *Bull. Am. Phys. Soc.* 41(10): 1834 (1997); A. Pizzuto, G. Mazzone, B. Coppi, "Halo Current Effects on Ignitor Plasma Chamber," *Bull. Am. Phys. Soc.* 41(10): 1834 (1997); M. Haegi, The Ignitor Group, "Diagnostic Systems for Ignitor," *Bull. Am. Phys. Soc.* 41(10): 1834 (1997); F. Bombarda, P. Buratti, and B. Coppi "Relevance of Present Reverse Shear Experiments to Ignitor," *Bull. Am. Phys. Soc.* 41(10): 1835 (1997); P. Detragiache, "Self-Consistent Analysis of n=1 Internal Mode Stability in Ignitor," *Bull. Am. Phys. Soc.* 41(10): 1835 (1997).

Recent results from active experiments, in particular from the high field machines, have been analyzed to provide useful information on the plasma characteristics typical of ignited regimes. Of special interest to our group have been the reverse shear experiments carried out on Alcator C-Mod at MIT and on the FTU machine at Frascati. The possibility of injecting high level of RF power in the very early phase of the discharge, with the purpose of controlling the current profile, has been verified. The nature and the characteristics of the associated MHD activity, and their possible extrapolation to the Ignitor range of plasma parameters is under investigation.

One recent result that we have obtained on ignition[47] concerns the possibility of using the enhanced confinement that has been observed to be associated with reversed shear profiles (nonmontonic current density profiles) in neutral beam heated experiments for ignition. There, improvements in the energy confinement time of a factor of 2-3 were observed. This regime would complement the conventional ignition scenario at high magnetic field and density, since it allows operation at lower current and density. The lower current has the advantage of being easier to maintain for longer periods of time, given the fixed capacity of the magnets in the machine, and therefore allows longer ignited plasma discharges.

As a longer term project, we are continuing to develop a potential design for an advanced fusion experiment that will burn D and ^{3}He, the Candor,[48] in a combined program of physics and engineering that parallels the Ignitor design for D-T. The proposed design has a similar maximum toroidal field to the Ignitor, in a larger plasma R $\simeq$ 1.8–2.2 m) that can support a larger current ($I_p \simeq$ 18 MA). Normally conducting magnets are envisioned for the toroidal field coils and a number of the engineering solutions developed for the Ignitor magnets and coils have been adapted for Candor. Numerical simulations[49]

emphasize that the most important property of D-^{3}He ignition is its strong time dependence and dynamic nature, even more so than D-T ignition. A large number of questions remain to be answered in both physics and the engineering design.

1.2.3 Emission above the Ion Cyclotron Frequency Induced by Fusion Reaction Products

D-T experiments[50] carried out by the JET and the TFTR machines have produced plasmas where a significant population of high energy α-particles are present. An important source of information on their distribution is the spectrum of radiation emission in the range of the α-particle cyclotron frequency and above. We have developed a theory for this emission based upon the excitation characteristics of a class of toroidal modes that we refer to as "contained modes."[51] Plasma inhomogeneity and magnetic field geometry play a key role in the structure of these modes,[52] which are radially localized versions of the magnetosonic-whistler wave. The α-particles resonate with the contained modes at harmonics of their cyclotron frequency. This frequency has a significant variation as a function of the distance from the symmetry axis where the magnetic field is evaluated.

The observed spectrum of radiation emission, which has a discrete part and a continuum, is consistent with our theory, in particular for the resonant frequency at which distinct peaks in the spectrum occur, and for the harmonic number above which the continuum spectrum is observed in experiments ($\omega \geq 8\Omega_c$, as estimated from observations in the JET experiments).

The results of our analysis of the excitation of the contained mode by α-particles have been accepted for publication in *Annals of Physics*. To complement

47   M.-H. Kuang, *D-T Ignition in the ITER and Ignitor Experiments*, B.S. thesis, Department of Physics, MIT, 1997; L.E. Sugiyama, "Reversed Shear Ignition for High Field Tokamaks," *Proceedings of the 23rd European Physical Society Conference on Controlled Fusion and Plasma Physics*, Kiev, Ukraine, 1996.

48   B. Coppi, *Physica Scripta* T2:2: 592 (1982); B. Coppi, *Nucl. Instr. Methods Phys. Research* A271: 2 (1988).

49   B. Coppi and L.E. Sugiyama, Questions in Advanced Fuel Fusion, RLE PTP-88/6 (Cambridge: MIT Research Laboratory of Electronics, 1988).

50   G.A. Cottrell, V.A. Bhatnagar, O. Da Costa, R.O. Dendy, J. Jacquinot, K.G. McClements, D.C. McCune, M.F.F. Nave, P. Smelders, and D.F.H. Start, "Ion Cyclotron Emission Measurements During JET Deuterium-tritium Experiments," *Nucl. Fus.* 33(9): 1365-87 (1993); S. Cauffman, and R. Majeski, "Ion Cyclotron Emission on the Tokamak Fusion Test Reactor," *Rev. Sci. Instrum.* 66(1): 817-19 (1995).

51   B. Coppi, G. Penn, and C. Riconda, "Excitation of Contained Modes by High Energy Nuclei and Correlated Cyclotron Emission," *Ann. Phys.* 261(2): 117-62 (1997).

52   B. Coppi, "Origin of Radiation Emission Induced by Fusion Reaction Products," *Phys. Lett. A* 172(6) 439-42 (1993).

the analytical calculations of the properties of the contained mode, we have also performed a study of the numerical solutions to the mode equation.

Current research is being done on the transport of α-particles in fusing plasmas, in particular through interactions with the contained mode. One aim of this research is to evaluate the possibility of experimentally interfering with the α-particle distribution by launching radio frequency waves that can couple to the described modes. Such effects would be limited to those energetic particles which reach the typical surface of localization of these modes towards the outer edge of the plasma.

The excitation of these modes by the injection of ion cyclotron waves (ICRF) is also being considered as a possible mechanism for the onset of toroidal rotation in plasmas subjected to balanced ICRF inputs. This toroidal rotation has been observed in both Alcator C-Mod[53] and JET.[54]

1.2.4 Interchange Instabilities in a Partially Ionized Plasma

The general theory of instabilities in partially ionized plasmas, where the ions and neutral atoms interact, is still in a relatively undeveloped state. It is known that neutrals can act to destabilize ion-dominated instabilities. For example, the dissipation provided by ion-neutral collisions can provide the outlet that allows modes to grow.[55] Another effect is the enhancement in the effective gravity that a neutral flow down the plasma density gradient can provide. We have considered[56] a simple problem that illustrates the second case. It is applicable to interchange modes in the edge region of magnetically confined plasmas and also to space physics, for example the heliosphere. The formulation enables the complex physics of finite neutral mean free path and self-consistent neutrals perturbations to be treated in a simple manner for the first time.

The basic physical picture can be understood from the fluid equations for the neutrals and ions, neglecting temperature perturbations. The momentum equations are

$$Mn_i\frac{dV_i}{dt} = -\nabla p_i + en_i\left(E + \frac{V_i \times B}{c}\right) \quad (42)$$

$$+ MN\nu_{ni}(V_n - V_i) - \nabla \cdot \Pi_i$$

$$MN\frac{dV_n}{dt} = -\nabla p_n + MN\nu_{ni}(V_i - V_n) - \nabla \cdot \Pi_n \quad (43)$$

where n_i is the ion density and N the neutral density, M the ion and neutral mass, V_i and V_n the ion and neutral velocities, ν_{ni} the neutral-ion collision frequency, and Π_i, Π_n the respective viscous stress tensors. Ionization and recombination are neglected.

The viscous stresses can be approximated as $\nabla \cdot \Pi \simeq Mn\nu\lambda_{mfp}^2\nabla_\perp^2 V$, where the collision frequency ν and the collisional mean free path λ_{mfp} are chosen to be appropriate to the species and regime. The ion viscous stress is due mainly to ion-ion collisions and the neutral viscous stress to charge exchange with the ions. The role of the viscous stresses is primarily to ensure that the relative velocities of the ions and neutrals remain small in equilibrium, $(V_n-V_i) \sim (\lambda_{ni}/L)^2$, where λ_{ni} is the neutral mean free path due to collisions with the ions and L is an equilibrium scale length. A nonzero neutral pressure gradient is required in equilibrium to drive the relative velocities.

Consider a simple 1D equilibrium with a main magnetic field B_{oz} in the z-direction and variation along the x-coordinate. Assume first that the neutrals themselves are immobile. (This corresponds to a large neutral viscosity, which rapidly dissipates the neutral perturbations.) The force exerted by the neutral flow on the ions, $F_x = Mn_i\nu_{in}V_{nx}$, acts like an effective gravity for the ions, $g = \nu_{in}V_{nx}$, that drives an interchange-like mode. It gives rise to an ion drift $V_{dy} = F_x \times B_{oz}$, which creates a charge separation in the x-direction, which in turn drives a y-drift $E_x \times B_{oz}$ that reinforces

53   J.E. Rice, M.J. Greenwald, I.H. Hutchinson, E.S. Marmar, Y. Takase, S.M. Wolfe, and F. Bombarda, "Observations of Central Toroidal Rotation in ICRF Heated Alcator C-Mod Plasmas," MIT Report PSFC/JA-97-4, submitted to *Nucl. Fus.*

54   L.-G. Eriksson, E. Righi, and K.-D. Zastrow, "Toroidal Rotation in ICRF-heated H-modes on JET," *Plas. Phys. Cont. Fus.* 39(1): 27-42 (1997).

55   B. Basu and B. Coppi, *Geophys. Res. Lett.* 15: 417 (1988); *J. Geophys. Res.* 94: 5316 (1989).

56   W. Daughton, P. Catto, B. Coppi, and S.I. Krasheninnikov, "Interchange Instabilities in a Partially Ionized Plasma," *Phys. Plas.*, forthcoming.

the perturbation. The collisional interchange growth rate has the form[57] $\gamma_o = g/(v_{in}L_i)$, where L_i is the ion pressure gradient scale length.

Solutions in two limits of v_{ni} are known for interchange-like modes:

6. strong neutral-ion collisionality, where v_{in} dominates, the ion-neutral flow gives the effective gravity above and the dispersion relation becomes $(\omega - iv_{in})(\omega - \omega_{*i}) = -(g/L_n)$. Here ω_{*i} is the ion diamagnetic drift frequency. The right hand side, $g/L_n = \gamma_{RT}^2$, is the square of the MHD Rayleigh-Taylor instability growth rate.

7. for small v_{ni}, the effect of neutrals disappears, and the ion viscosity modifies the growth rate,[58] $(\omega - i(v_{ii}/8)k_\perp^2\rho_i^2)(\omega - \omega_{*i}) = -(g/L_n)$ where v_{ii} is the ion-ion collision frequency and $k_\perp$ the wave number perpendicular to the magnetic field, and ρ_i the finite ion Larmor radius. The factor 1/8 is due to detailed considerations.[59] The growth rate then becomes

$$\gamma = \gamma_0/(1 + (v_{ii}/8)k_\perp^2\rho_i^2).$$

The case of interest is the regime of intermediate ion-neutral collisionality, where the mean free path of the neutrals due to collisions with the ions, λ_{ni}, is finite, though small compared to the plasma scale lengths. Here the fluid model and the simple fluid viscosity are no longer valid. On the other hand, combining the two known limits and the role played by the viscous stresses, we expect a form

$$(\omega - iv_{in}k_\perp^2\lambda_{mfp}^2)(\omega - \omega_{*i}) = -(g/L_n). \tag{44}$$

Thus the growth rate should show a substantial reduction from the ideal growth rate given in case 1, with the approximate form

$$\gamma = \gamma_{RT}\frac{v_{in}G}{v_{in}G + k_\perp^2\rho_i^2v_{ii}/8} \tag{45}$$

that represents the smooth connection of the two limiting cases. Here G is a function of plasma parameters that reduces to 1 for small $v_{ni}/k_\perp v_{thi} \ll 1$ and

$(1/2)(k_\perp^2 v_{thi}^2/v_{ni})$ in the opposite limit. This form also shows that the effect of allowing self-consistent perturbations of the neutrals' velocity by the instability can be modeled by the simple substitution $v_{in}G$ for v_{in}, where $G \simeq 1 + Z$ is a function of the plasma parameters.

Detailed analysis[60] confirms the usefulness of the simple form for describing the growth rate and effects of perturbations in the neutral flow.

1.2.5 Sawtooth Oscillations in Alcator C-Mod

The Alcator C-Mod experiment has been operating for several years at MIT. It is dedicated to the physics of advanced plasma regimes, including operation at high magnetic fields, radio frequency (RF) heating of high density plasmas, and the optimization of divertors. It has many of the characteristics of planned ignition experiments such as plasma shaping, well thermalized plasmas with $T_e \geq T_i$, high power densities and pressures, and the ability to explore a relatively wide range of regimes.

In collaboration with the Alcator group, we are engaged in a general study of instability regimes in Alcator C-Mod plasmas. An important part of this study involves understanding the sawtooth activity as a function of plasma parameters (i.e., density, temperatures, current, magnetic field, auxiliary heating power). Sawteeth are almost always present in the plasmas produced by this machine. Their period is largely independent of operating density and increases as RF heating is applied and the contained energy is increased. The sawtooth amplitude is seen to saturate as the period increases and precursor oscillations, with dominant poloidal mode number m = 1, are commonly observed in that case. One can probably understand this by noting that on Alcator C-Mod the ohmic power increases with density (approximately to the 1/2 power), while the stored energy remains roughly constant.[61]

We have analyzed about 300 discharges/time slices to derive the significant trends of the sawtooth behavior and for a smaller number (~ 30) we have

57 J. Dungey, *J. Atmos. Terr. Phys.* 9: 304 (1956).

58 B. Coppi, in *Nonequilibrium Thermodynamics* (Chicago: The University of Chicago Press, 1965).

59 Ibid.

60 W. Daughton, P. Catto, B. Coppi, and S.I. Krasheninnikov, "Interchange Instabilities in a Partially Ionized Plasma," *Phys. Plasmas*, forthcoming.

run a more detailed linear stability analysis. The saw-tooth period varies between approximately 4 msec, in ohmic low current plasmas, and 27 msec in RF heated H-mode discharges. The onset of sawtoothing activity generally takes place at about 200 msec after the plasma breakdown. A list of significant geometrical and plasma parameters for Alcator C-Mod is given in Table 3 (note that most of the discharges analyzed were with magnetic field $B_T \simeq 5.3T$). It can be observed that for this machine the current diffusion times are considerably longer (ranging from 100 msec to well over 1 sec) than the sawtooth period, and the latter is always shorter than the energy confinement time (30-80 msec, typically).

Table 3: Alcator C-Mod main parameters

$B_T = 3.5 \rightarrow 7.8T$	$a = 20 \rightarrow 22$cm
$R \approx 67$cm	$r_1 = r(q = 1) = 5 \rightarrow 9$cm
$\kappa = 1.0 \rightarrow 1.7$(ellipticity)	$\delta = 0 \rightarrow 0.6$(triangularity)
$\omega_{*e} = (0.8 \rightarrow 7.7) \times 10^4 \sec^{-1}$	$\tau_A = (0.2 \rightarrow 1.7) \times 10^{-6} \sec$
$T_e/T_i = $ $(1.0 \rightarrow 2.0)$(Ohmic)sec^{-1}	$\nu_{ei} = (0.5 \rightarrow 5.2) \times 10^5 \sec^{-1}$
$T_e/T_i = $ $(0.8 \rightarrow 1.4)$(RF – heated)	

The ideal-MHD stability of Alcator C-Mod plasmas has been explored for the (toroidal) n = 1 mode using the PEST-1 numerical code.[62] From the reconstructed profiles of q(r) (related to the inverse rotational transform) and p(r) (plasma pressure), as well as knowledge of the plasma shape, this code computes the linear stability properties of these modes, that are driven by the plasma pressure gradient. Our conclusion is that all discharges analyzed so far appear to lie in the region of ideal stability, $\beta = 8\pi p/B^2$ < β_{crit}, by a comfortable margin (roughly a factor of 2). A rudimentary "error analysis" has been carried out by varying the shape of the input q-profile and shows

that this causes the value of β_{crit} to change little: we have varied s_1, the local value of the magnetic shear at the q = 1 surface, by ±26% and β_{crit} changed only by some 6%. Hence, it is apparent that sawteeth in Alcator C- Mod are not due to an ideal internal kink (n = m = 1) mode, but are likely related to resistive instabilities.

It should be pointed out that the central β in Alcator C-Mod is considerably lower than the values expected in ignition experiments. This means that the Alcator produced C-Mod plasmas are generally ideal MHD stable, even for low values of q_a. The relatively small size of the $q \leq 1$ volume also contributes to stability. Ignition experiments require higher central pressures. For the reference parameters of the Ignitor experiment, for example, $p_0 \simeq 4.2$ MPa, and $\beta_0 \simeq 5.5\%$.

We have begun the analysis of resistive modes in the Alcator C-Mod produced plasmas by looking at the theoretical predictions of two-fluid theory.[63] Initial estimates show a good correlation between the morphology of sawteeth (short versus long period) and their occurrence (or absence) and the theoretically predicted marginal stability curve. Long period sawteeth appear to be correlated with a relatively large value of the normalized diamagnetic frequency, $\omega_{*e}\tau_A/\varepsilon_\eta^{1/3}$, a behavior that can be qualitatively predicted from the theory. Here $\omega_{*e} = -(c/eBnr)(dp_e/dr)$, $\tau_A = \sqrt{3}R/V_A$, where V_A is the Alfvén speed, and $\varepsilon_\eta = (1/2)(c/\omega_{pe}r_1)^2\nu_{ei}\tau_A$, where r_1 is radius of the q = 1 surface.

Efforts are underway to put this work on a firmer basis, via a collaboration with the theoretical team of JET (Joint European Torus, U.K.). We will use their resistive, toroidal code CASTOR[64] to obtain a more accurate estimate of the growth rate of resistive internal n = 1 modes. This will provide, for the first time, a systematic description of resistive instabilities in a

61 B. Coppi, S. Migliuolo, L.E. Sugiyama, F. Bombarda, and P. Detragiache, "Evolution of Global Modes and Magnetic Reconnection in Fusion Burning Plasmas," *Proceedings of the 16th international IAEA Conference on Fusion Energy* 2: 397, Montreal, Canada, October 1996 (Vienna, Austria: International Atomic Energy Agency, 1997).

62 R.C. Grimm, R.L. Dewar, J. Manickam, "Ideal MHD Stability Calculations in Axisymmetric Toroidal Coordinate Systems," *J. Comp. Phys.* 49: 94 (1983).

63 B. Coppi, R. Galvão, R. Pellat, M.N. Rosenbluth, and P.H. Rutherford, "Resistive Internal Kink Mode," *Sov. J. Plasma Phys.* 2: 533 (1976); G. Ara, B. Basu, B. Coppi, G. Laval, M.N. Rosenbluth and B.V. Waddell, "Magnetic Reconnection and m = 1 Oscillations in Current Carrying Plasmas," *Ann. Phys.* (NY) 112: 443 (1978).

64 W. Kerner, J.P. Goedbloed, G.T.A. Huysmans, S. Poedts, and E. Schwartz, "CASTOR: Normal Mode Analysis of Dissipative MHD Plasmas," *Joint European Torus Report* JET- P(97)04 (Abingdon, U.K.: JET Joint Undertaking, 1997).

high particle and power density shaped plasma and afford some valuable insight on future ignition experiments.

1.2.6 Composite Transport Coefficients for Well-Confined Plasmas

A plasma energy confinement scaling and its associated transport coeffient has been generalized from the experiments carried out by the Alcator C-Mod machine at MIT to explain the observed confinement in experiments carried out by other machines.[65] The transport results from a competition between the usual outward diffusive transport of energy, down the temperature (pressure) gradient, and a process that reduces the outward flux. Theoretically, it follows arguments based on the symmetry properties of a proposed transport matrix,[66] where both the temperature and the toroidal plasma current, which provides the reduction effect, are taken into account. The resulting scaling for the total energy confinement time is not a simple power law scaling, but is composed of two terms. It successfully fits discharges from the D-III D, JET, JT-60, PDX, TFTR, and FTU machines, collected in the ITER project experimental database.

The scaling arose from observations of ohmic and ICRF-heated plasmas in Alcator C-Mod.[67] For ohmic discharges, it was observed that $\beta_p/q_E^{2/3}$ was roughly constant ($\beta_p = 2\mu_0 p/B_p^2$, based on the poloidal field at the outer edge of the plasma column, and $q_E \equiv 2\pi a^2 \kappa B_T/(\mu_0 I_p R)$. Since one expects that the plasma pressure, and thus β_p should increase with the applied heating power, a natural generalization to consider is the ratio of the total plasma heating power P_H to a characteristic heating power. For ohmically heated plasmas, the characteristic power scaling is the product of the toroidal plasma current I_p and a characteristic scaling for the toroidal loop voltage V_0. The voltage is a natural parameter for the ohmic power scaling, since it does not vary greatly between

different discharges and different machines. On the other hand, for auxiliary heated discharges the voltage varies widely and another scale must be found.

For ohmic plasmas, previous work in theory and experiment suggests that the dimensionless coefficient on which the CMG diffusion coefficient[68] is based can be used to identify a characteristic loop voltage

$$V_0 = \alpha_V \frac{T_e}{e} \left(\omega_{pi} \frac{c^2}{\omega_{pe}^2} \frac{v_e}{v_{the}^2} \right)^{2/5}, \qquad (46)$$

where α_V is a numerical constant chosen so that $V_0 \simeq 1$ Volt for typical parameters in tokamak-like machines, ω_{pi} and ω_{pe} are the ion and electron plasma frequencies, v_e the electron collision frequency, and v_{the} the electron thermal velocity. Ohmic data from Alcator C-Mod shows that $\beta_p/q_E^{2/3}$ is well represented by the linear relation

$$\beta_p/q_E^{2/3} \approx \gamma_1 \frac{P_H}{I_p V_0} + \gamma_2, \qquad (47)$$

where the two terms make roughly equal contributions, and γ_1 and γ_2 are almost constant.

A more general form can be used to describe auxiliary heated plasmas,

$$\beta_p/q_E^{2/3} \approx f_1 \frac{P_H}{I_p V_0} + f_2, \qquad (48)$$

where f_1 and f_2 are functions of dimensionless parameters involving geometry and other global plasma parameters, which have been estimated from experimental data.

The L-mode data base assembled for the ITER project was used to find possible functional forms for f_1 and f_2. Plasmas, like those produced by Alcator C-Mod, that are clean and close to thermodynamic

65 B. Coppi and W. Daughton, "Composite Transport Coefficients for Well Confined Plasmas," *Proceedings of the 24th European Physical Society Conference on Controlled Fusion and Plasma Physics*, Berchtesgaden, Germany, June 1997; W.S. Daughton, *Transport Processes in Well Confined High Temperature Plasmas and Collective Modes in their Partially Ionized Edge Region*, Ph.D. diss., Department of Physics, MIT, 1998.

66 B. Coppi and F. Pegoraro, *Phys. Fluids B* 3: 2582 (1991).

67 B. Coppi and W. Daughton, "Composite Transport Coefficients for Well Confined Plasmas," *Proceedings of the 24th European Physical Society Conference on Controlled Fusion and Plasma Physics*, Berchtesgaden, Germany, June 1997; W.S. Daughton, *Transport Processes in Well Confined High Temperature Plasmas and Collective Modes in their Partially Ionized Edge Region*, Ph.D. diss., Dept. of Physics, MIT, 1998.

68 B. Coppi and E. Mazzucato, *Phys. Lett. A* 71: 337 (1979).

equilibrium were chosen, including both ohmic and auxiliary heated L-mode cases. Plasmas of this kind are most relevant to fusion ignition conditions.

An additional weak density dependence was grouped into a modified voltage scaling V_0°,

$$V_0^\circ \approx V_0\left(\frac{v_*}{1+v_*} + \frac{n_0^{o\,1/3}}{n}\right), \tag{49}$$

where the constant $\alpha_V = 0.18$ in the original scaling and $(n_0^o/n)^{1/3} \equiv C_1(\omega_{pi}/v_e)^{2/3}(c/4\pi v_{the})^2(m_e/m_p)$, where the constant $C_1 \approx 0.24$. Power law forms for f_1 and f_2 were found to be

$$f_1 \approx 0.11(d_i/a)^{1/3}A_i^{1/4}(\omega_{pe}/\Omega_{ce})^{1/3}$$ and

$$f_2 \approx 0.15(R/10a)A_i^{1/2}(\omega_{pe}/\Omega_{ce})^{1/3},$$ where A_i is the average atomic mass number, the ion skin depth $d_i = c/\omega_{pi}$ is evaluated with the line-average electron density, and Ω_{ce} is the electron gyro-frequency.

As a consequence, the energy confinement time τ_E, where $dW/dt = W/\tau_E$ for the total plasma thermal energy W, does not have a simple power law scaling, but varies as

$$\tau_E \approx 0.031Rq_E^{2/3}I_p\left(1 + f_3\frac{I_pV_0^\circ}{P_H}\right)\left(\frac{d_i}{a}\right)^{1/2}\left(\frac{\omega_{pe}}{\Omega_{ce}}\right)A_i^{1/4}, \tag{50}$$

with R in meters, I_p in MA, P_H in MW, and τ_E in seconds. The term containing $f_3 \approx 1.4(R/5a)^{1/2}(R/20d_i)^{1/2}A_i^{1/4}$ represents the reduction in the outward thermal transport. It can be seen that the typically observed decline in confinement with increasing total heating power results from the reduction in this term. In marked contrast to the more familiar L-mode confinement scalings, which are strict power laws, this one predicts that the confinement time will saturate at large values of the heating power, rather than continuously decline.
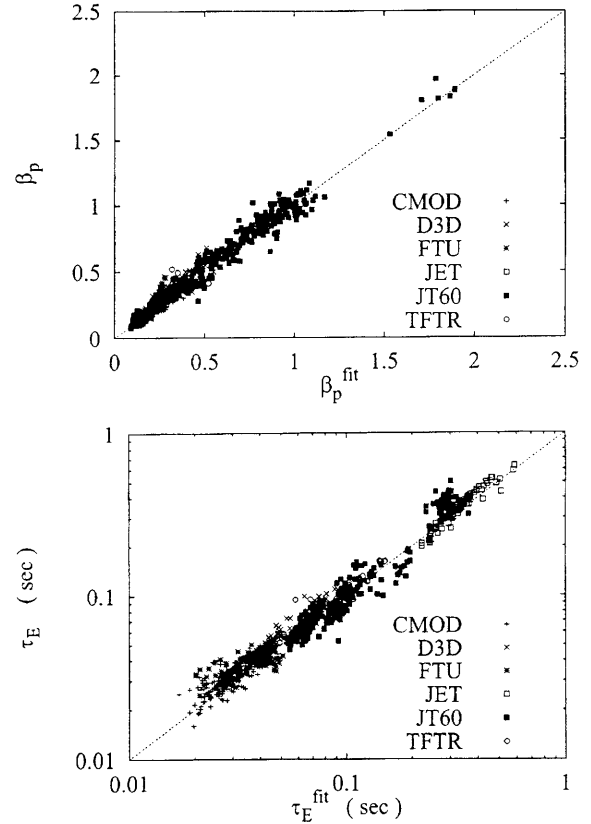

Figure 21. Comparison of the β_p and τ_E scalings with experimental data.

A thermal transport coefficient that incorporates the ideas expressed above can be written in terms of the properties of "ubiquitous" modes driven by the electron pressure gradient. Then β_p is replaced by $\beta_{p*} \equiv 2\mu_0 p_{e*}/B_p^2$, where $p_{e*} \equiv |dp_e/dr|_{max}a_p$, the maximum pressure gradient over the plasma cross-section, where a_p is the radius of the maximum gradient. A number of numerical simulations using a 1 1/2 D transport code show good agreement with Alcator C-Mod electron temperature profiles over a range of discharges.[69]

69   B. Coppi and W. Daughton, "Composite Transport Coefficients for Well Confined Plasmas," *Proceedings of the 24th European Physical Society Conference on Controlled Fusion and Plasma Physics*, Berchtesgaden, Germany, June 1997; W.S. Daughton, *Transport Processes in Well Confined High Temperature Plasmas and Collective Modes in their Partially Ionized Edge Region*, Ph.D. diss., Department of Physics, MIT, 1998.

1.2.7 Two-Fluid and Parallel Compressibility Effects in Tokamak Plasmas

The MHD, or single fluid, model for a plasma has long been known to provide a surprisingly good description of the observed nonlinear dynamics of confined plasmas, considering its simple nature compared to the complexity of the real system. On the other hand, some of the supposed agreement arises from the lack of the detailed measurements that are needed to distinguish MHD from more sophisticated models. At present, a number of factors combine to make models beyond MHD of practical interest. Computational considerations still favor fluid rather than particle models for description of the full plasma, and suggest a two-fluid approach that extends MHD to slower time scales and more accurate parallel dynamics.

We have used a set of two-fluid (electron and ion) equations for toroidal (tokamak) geometry to develop MH3D-T code.[70] The code and its original MHD version, MH3D[71] are the first numerical, initial value models in toroidal geometry that include the full 3D (fluid) compressibility and electromagnetic effects. Previous nonlinear MHD codes for toroidal geometry have, in practice, neglected the plasma density evolution, on the grounds that MHD plasmas are only weakly compressible and that the background density variation is weaker than the temperature variation. For two-fluid plasmas, the density evolution

provides the basic driving energy for the diamagnetic drifts of the electrons and ions perpendicular to the magnetic field. Work with MH3D-T has shown that the density evolution is also crucial in MHD, since it strongly influences the parallel dynamics, in combination with the parallel thermal conductivity. The true parallel plasma dynamics are driven by additional kinetic processes that are not included in the fluid picture, but the basic fluid effects remain and should be understood first.

The two-fluid code is part of a larger project, the 3D, or Multi-Level 3D project[72] for toroidal plasmas. Its goal is to develop a comprehensive suite of simulation models that cover a range of physics from simple to complex, starting from the fluid and progressing toward kinetic models. In addition to the new physics that it describes, MH3D-T provides a good base for adding additional, non-fluid effects in a fully electromagnetic and toroidal model. Recent studies with MH3D-T have involved adding the $(p_\parallel - p_\perp)$ effects of neoclassical MHD[73] in the momentum stress tensors.[74] A gyrokinetic particle simulation for the ions has recently been combined with electron fluid model of MH3D-T.[75] The GK ion model is collisionless, allowing different regimes to be treated.

The two-fluid equations used in MH3D-T are based on the drift ordering,[76] which has been generalized to arbitrary perturbation size. This ordering contains time scales slower than MHD ($\partial/\partial t \sim \delta v_{th}$, where δ

70 L.E. Sugiyama and W. Park, *A Two-Fluid Model for Toroidal Plasmas*, RLE PTP-96/2 (Cambridge: MIT Research Laboratory of Electronics, 1997); L.E. Sugiyama, "Two-Fluid Toroidal Effects in Tokamak Plasmas," *Proceedings International Workshop on Nonlinear and Extended MHD*, Madison, Wisconsin, 1997, Center for Plasma Theory and Computation Report UW-CPTC 97-5 (Madison, Wisconsin: University of Wisconsin, 1997); L.E. Sugiyama and W. Park, "Two-Fluid and Parallel Compressibility Effects in Tokamak Plasmas," invited paper presented at *2nd Asian Plasma Physics and Theory Conference*, Toki, Japan, October 1997, forthcoming; L.E. Sugiyama, W. Park, "Plasma Rotation in Two-Fluid Tokamaks," *Bull. Am. Phys. Soc.* 42(10): 1854 (1997).

71 W. Park and D.A. Monticello, *Nucl. Fusion* 30: 2413 (1990); W. Park, D.A. Monticello, H. Strauss, J. Manickam, *Phys. Fluids* 29: 1171 (1986).

72 W. Park, S. Parker, H. Bigliari, M. Chance, L. Chen, C.Z. Cheng, T.S. Hahm, W.W. Lee, R. Kulsrud, D. Monticello, L. Sugiyama, and R. White, *Phys. Fluids B* 4: 2033 (1992); W. Park, E.V. Belova, G.Y. Fu, H.R. Strauss, L.E. Sugiyama, "M3D (Multi-level 3D) Project for Simulation of Plasmas," *Bull Am. Phys. Soc.* 42(10): 1854 (1997); W. Park, G.Y. Fu, H.R. Strauss, L.E. Sugiyama, *Proceedings Int. Workshop on Nonlinear and Extended MHD*, Madison, Wisconsin, 1997, *Center for Plasma Theory and Computation Report* UW-CPTC 97-5 (Madison, Wisconsin: University of Wisconsin, 1997); W. Park,......, L.E. Sugiyama, "3D Simulation Studies of Tokamak Plasmas using MHD and Extended-MHD Models," *Proceedings of the 16th International IAEA Conference on Fusion Energy* 2: 411, Montreal, Canada, October 1996 (Vienna, Austria: International Atomic Energy Agency, 1997); H.R. Strauss, W. Park, G.Y. Fu, and E. Belova, "Unstructured Mesh 3D MHD Simulations with MH3D++," *Bull Am. Phys. Soc.* 42(10): 1854 (1997); E.V. Belova, W. Park, G.Y. Fu, H.R. Strauss, and L.E. Sugiyama, "3D Hybrid Simulations with Gyrokinetic Particle Ions and Fluid Electrons," *Bull Am. Phys. Soc.* 42(10): 1854 (1997).

73 S.P. Hirshman and D. Sigmar, *Nucl. Fus.* 21: 1079 (1981); J.D. Callen and K.C. Shaing, *Phys. Fluids* 28: 1845 (1985).

74 L.E. Sugiyama, W. Park, "Plasma Rotation in Two-Fluid Tokamaks," *Bull Am. Phys. Soc.* 42(10): 1854 (1997).

75 E.V. Belova, W. Park, G.Y. Fu, H.R. Strauss, and L.E. Sugiyama, "3D Hybrid Simulations with Gyrokinetic Particle Ions and Fluid Electrons," *Bull Am. Phys. Soc.* 42(10): 1854 (1997).

76 R.D. Hazeltine and J.D. Meiss, *Phys. Rep.* 121: 1 (1985), and in *Plasma Confinement*, (Redwood City, California: Addison-Wesley Publishing Company, The Advanced Book Program, 1992).

is a small parameter and v_{th} is the ion thermal velocity), while retaining validity beyond the strictly collisional regime, but it is not rigorous nonlinearly. Electrons and ions are treated as separate fluids. The model includes the ion gyroviscous force, the Hall terms and electron pressure gradient in Ohm's law, and equations for the electron and ion temperature evolution, with parallel and perpendicular thermal conductivities. As a first approximation, the electrons are treated as massless and the pressures assumed to be isotropic.

The fluid velocities can be written exactly in terms of the generalized diamagnetic velocities as $\mathbf{v}_i = \mathbf{v} + \mathbf{v}_{di}$ and $\mathbf{v}_e = \mathbf{v} + \mathbf{v}_{*e} - \mathbf{J}_{\parallel}/en_e$, where $\mathbf{v}_{*j} \equiv \mathbf{B} \times \nabla p_j/(q_j n_j B^2)$. The perpendicular ($\perp$ $\mathbf{B}$) component of $\mathbf{v}$ is the guiding center velocity of the electrons and ions in the perpendicular direction. The generalized ion diamagnetic velocity $\mathbf{v}_{di} \equiv \mathbf{J}_{\perp}/(en_e) + \mathbf{v}_{*e}$ contains the polarization drift.

In terms of v, the two-fluid equations can be written in rationalized units as

$$\frac{\partial \mathbf{v}}{\partial t} + (\mathbf{v} \cdot \nabla)\mathbf{v} =$$
$$-(\mathbf{v}_{di} \cdot \nabla)\mathbf{v}_{\perp} + \frac{\mathbf{J} \times \mathbf{B}}{\rho} - \frac{\nabla p}{\rho} + \mu \nabla^2 \mathbf{v} + \frac{V_{gv}}{\rho} - \frac{\nabla \cdot \Pi_{i\parallel}}{\rho} \tag{51}$$

$$\frac{\partial \mathbf{B}}{\partial t} = -\nabla \times \mathbf{E} \tag{52}$$

$$\mathbf{E} = -\mathbf{v} \times \mathbf{B} + \eta \mathbf{J}^* - \frac{\nabla_{\parallel} p_e}{en} - \frac{\nabla \cdot \Pi_{e\parallel}}{en} \tag{53}$$

where $\mathbf{J}^* = \mathbf{J} + (3/2)en\mathbf{v}_{*Te}$. Here ρ is the plasma mass and V_{gv} represents the parallel vorticity-related part of the ion gyroviscous force

$$\nabla \cdot \Pi_i^{gv}, V_{gv} = -[(\nabla_{\perp} + 2\hat{\mathbf{b}}\nabla_{\parallel})X \tag{54}$$
$$+ (p_i/\Omega_{ci})(\hat{\mathbf{b}} \times \nabla_{\perp})\nabla_{\parallel}\mathbf{v}_{i\parallel}]$$

with $X \equiv -(p_i/2\Omega_{ci})\hat{\mathbf{b}} \cdot \nabla \times \mathbf{v}_{i\perp}$. The continuity and temperature equations ($p_j = N_j T_j$, $n_e = n_i \equiv n$) are, with $\nabla \cdot \mathbf{J} = 0$,

$$\frac{\partial n}{\partial t} + \nabla \cdot (n\mathbf{v}_e) = 0 \tag{55}$$

$$\frac{\partial T_j}{\partial t} + \mathbf{v}_j \cdot \nabla T_j = -\hat{\Gamma}_j T_j \nabla \cdot \mathbf{v}_j \tag{56}$$
$$+ \nabla \cdot n\kappa_{\perp j}\nabla_{\perp}T_j + \nabla \cdot n\kappa_{\parallel j}\nabla_{\parallel}T_j - \hat{\Gamma}_j \nabla \cdot (T_j \mathbf{v}_{*Tj})$$

for electrons and ions j = e,i, where $\hat{\Gamma}_j = \Gamma_j - 1$, Γ_j being the ratio of specific heats, and $\mathbf{v}_{*Tj}$ is the diamagnetic drift based on the temperature gradient. The neoclassical, collisional parallel viscous forces $\nabla \cdot \Pi_{j*}$, that extend the fluid model into the long parallel mean free path regime[77] are currently being tested.

Tests of the model showed a number of new and unexpected effects due primarily to the new introduced parallel dynamics; they are equally important in MHD.

The continuity equation for the ions (equation (55) with $\mathbf{v}_e$ replaced with $\mathbf{v}_i$) introduces the possibility of sound wave propagation along the magnetic field whenever the steady state condition $\nabla \cdot n\mathbf{v}_i$ is not satisfied. (The plasma mass velocity in equation (51), the total momentum equation, is mostly $\mathbf{v}_i$.) This propagation condition differs from that given by the pressure equation at fixed density. The parallel dynamics have much stronger effects in a torus than in a cylinder, due to the poloidal asymmetry of the flux surfaces, and also influence the poloidal plasma rotation and thereby the parallel flows through various forms of magnetic pumping.[78]

The numerical results clearly illustrate the competing effects of the density evolution and the parallel thermal conductivity. For linear resistive modes, the density evolution can be stabilizing or destabilizing. The strong stabilizing effect of the density equation on the m/n = 1/1 resistive mode in a torus with R/a = 3 has been shown for strongly and weakly ideal MHD unstable modes.[79] A factor of 2 reduction in growth rate was seen for the resistive modes with weaker original growth rates. In a cylinder the effect is also stabilizing, but much smaller.

77   S.P. Hirshman and D. Sigmar, *Nuclear Fusion* 21: 1079 (1981); J.D. Callen and K.C. Shaing, *Phys. Fluids* 28: 1845 (1985).

78   J.M. Berger, W.A. Newcomb, J.M. Dawson, E.A. Frieman, R.M. Kulsrud, A. Lenard, *Phys. Fluids* 1: 301 (1958); T.H. Stix, *Phys. Rev. Lett.* 16: 1260 (1973); A.B. Hassam and R. Kulsrud, *Phys. Fluids* 21: 2271 (1978).

The parallel thermal conductivity (stabilizing) and the density evolution have competing effects on other linear resistive modes in a torus. For the 3/2 resistive ballooning mode studied,[80] the perturbed pressure and velocity stream function $u(\mathbf{v} = \varepsilon R \nabla u \times \hat{\phi} + \nabla_{\perp \chi} + v_\phi \hat{\phi})$ appear similar for the case with no density evolution ($\partial n/\partial t = 0$) and $\kappa_{\parallel} = 0$ and for the case with both density evolution and relatively strong $\kappa_{\parallel}$. Turning on $\kappa_{\parallel}$ while keeping $\partial n/\partial t = 0$ decouples the perturbations on adjoining magnetic surfaces and stabilizes the mode, $\gamma < 0$. Turning on the density evolution from this state returns to the basic eigenfunction shape of the growing mode, but γ is reduced by 1/3.

Nonlinearly, the parallel dynamics described by the density equation also introduces important differences.[81] When the density evolves, both MHD and two-fluid magnetic islands are seen to couple much more easily to islands of different *toroidal* mode number n with fixed density. Thus a 2/1 island with evolving density triggered 3/2 and 4/3 islands, as well as the usual n = 1 set (3/1, 4/1, 5/1, etc.) that is expected from the toroidal mode coupling. With fixed density, the companion n = 1 islands developed in the same amount of time, while the n ≠ 1 islands remained very small. The two-fluid effects on island coupling were much smaller than those of the density evolution. They did seem to increase the coupling somewhat, and the various islands had different relative phases and poloidal rotations.

Plasma rotation in the poloidal direction is another topic that has important implications for stability and confinement that is poorly understood because it is difficult to treat in a full torus. In a cylinder, the poloidal rotation is not strongly constrained in the steady state because of the poloidal symmetry of the flux surfaces. A torus, however, resists poloidal rotation of the plasma, while the toroidal rotation is constrained to the form $v_\phi = R\Omega(\psi)$. (The ideal MHD

torus can have a nonzero parallel flow in addition, $\mathbf{v} = K(\psi)\mathbf{B}$, but the simulation results confirm that it is not robust under non-ideal conditions.) In addition to previously studied mechanisms for magnetic pumping, which require dissipation, such as viscosity, to remove the rotational energy,[82] the numerical simulation shows that the fluid parallel dynamics in a torus also tend to damp the ion poloidal rotation. The effect can be large at high rotation velocities. The two-fluid terms add other effects, including radial convection, and lead to steady states where the poloidal velocity of either the electron or ion fluid is zero in steady state and an electric potential across the plasma radius exists.[83] Simulation results so far support these expectations. Rotation including the neoclassical MHD effects are also currently under investigation.

When the density steady state $\nabla \cdot n\mathbf{v} \neq 0$, the poloidal velocity v_θ and the related toroidal velocity v_ϕ begin to oscillate on a fast (sound wave) time scale and the oscillations experience a outward radial propagation.

Two-fluid effects also have important stabilizing or destabilizing effects on mode stability. The most straightforward depend on the diamagnetic drifts of the electrons and ions, described by the ratio ω_{*i}/γ_0, where γ_0 is the growth rate without two-fluid effects. For reconnecting modes, the ion ω_{*i} is generally stabilizing and the electron ω_{*e} destabilizing. The latter causes a complex radial shearing of the electron motion (i.e., the current) in the reconnection layer. In addition, the sound speed gyroradius $\rho_s = v_s/\Omega_{ci}$ is always destabilizing. The two-fluid code demonstrates the stabilizing effect of ω_{*i} on the 1/1 resistive mode in a cylinder and also the general physical mechanism of ω_{*i}-stabilization for reconnecting modes of all m.[84] The ion ω_{*i} causing the plasma mass flow into the reconnection layer from the interior r < r_1 to rotate poloidally relative to the reconnec-

79 B. Coppi, S. Migliuolo, L.E. Sugiyama, F. Bombarda, P. Detragiache, "Evolution of Global Modes and Magnetic Reconnection in Fusion Burning Plasmas," *Proceedings of the 16th Int. IAEA Conference on Fusion Energy* 2: 397, Montreal, Canada, October 1996 (Vienna, Austria: International Atomic Energy Agency, 1997).

80 L.E. Sugiyama, "Two-Fluid Toroidal Effects in Tokamak Plasmas," *Proceedings Int. Workshop on Nonlinear and Extended MHD*, Madison, Wisconsin, 1997, Center for Plasma Theory and Computation Report UW-CPTC 97-5 (Madison, Wisconsin: University of Wisconsin, 1997); L.E. Sugiyama and W. Park, "Two-Fluid and Parallel Compressibility Effects in Tokamak Plasmas," invited paper presented at *2nd Asian Plasma Physics and Theory Conference*, Toki, Japan, October 1997, forthcoming.

81 L.E. Sugiyama and W. Park, *A Two-Fluid Model for Toroidal Plasmas*, RLE PTP-96/2 (Cambridge: MIT Research Laboratory of Electronics, 1997).

82 J.M. Berger, W.A. Newcomb, J.M. Dawson, E.A. Frieman, R.M. Kulsrud, and A. Lenard, *Phys. Fluids* 1: 301 (1958); T.H. Stix, *Phys. Rev. Lett.* 16: 1260 (1973); A.B. Hassam and R. Kulsrud, *Phys. Fluids* 21: 2271 (1978).

83 E. Bowers and N.K. Winsor, *Phys. Fluids* 14: 2203 (1971).

tion X-point in the ω_{*e} direction. This results from the perturbed $\tilde{v}_{*ir}$ part of the radial ion fluid velocity as ω_{*i} increases. When $\omega_{*e} = 0$, the rotation angle reaches approximately $\pi/2$ near $\omega_{*i}/\gamma_0 \simeq 2$, the point where the mode reaches the maximum stabilization, i.e., the inflow is almost exactly out of phase with the reconnection. If $\omega_{*e} \neq 0$, the perturbed current J_z in the reconnection layer also shears poloidally, and the relative inflow rotation angle and stabilization effect are reduced. The poloidal direction of the velocity component $\tilde{v}_{*ir}$ is always exactly out of phase with the X-point and has the same stabilizing effect at all m, for both cylinder and torus.

1.2.8 Fusion Ignition Using the Initial Current Ramp

Typical studies of the feasibility of fusion ignition in toroidal plasmas consider the plasma power balance in steady state. However, it has long been known that ignition must be a dynamic process and also that it is easiest to achieve when the plasma profiles are driven from their characteristic steady state forms.

For any tokamak-like toroidal confinement device, there is an initial stage between the formation of the plasma, at relatively low density and temperature and small internal toroidal current, and the final parameters. This initial 'current ramp' phase of rising plasma current and plasma density may constitute a substantial fraction of the discharge time. For fusion plasmas, it represents an important opportunity to raise the plasma temperature quickly, using comparatively little power, at densities that are lower than the final ones. Also, the current density can be 'frozen-in' to a relatively broad radial profile by lowering the resistive diffusion, where the resistivity varies as $T_e^{-3/2}$. The lowest deuterium-tritium (D-T) fusion temperatures of 12-15 keV, corresponding to high particle density, can significantly lower the diffusion rate in the plasma center, but it remains high in the outer region. Broad current profiles can prevent serious interior plasma instabilities, particularly if the magnetic safety factor q > 1 everywhere (q is proportional

to the inverse of the winding number of the magnetic field around the torus, the number of poloidal turns per toroidal circuit). The same advantages persist for ignition even in reactor designs, although the device actually runs for long periods in steady state.

We have previously shown,[85] using 1 1/2 D transport simulation, that toroidal plasmas with tight aspect ratio (small R/a ~ 3) at high magnetic field, current, and plasma density can benefit significantly from heating during the current ramp to reach ignition, reaching ignition shortly after the final current is attained and thus allowing almost the entire high current phase of the discharge to be used for the fusion. Here ignition is defined to be the point when the fusion heating takes over the maintenance of the plasma energy balance from externally applied heating sources. This gain in burning time is especially important in high field experiments, where the heating of the field magnets puts a stringent limit on the discharge duration. Plasma stability, in terms of q > 1, is also significantly improved. In addition, the broad current profile and non-relaxed profile of the toroidal loop voltage, which is correspondingly large toward the outside (r → a) of the plasma allow a substantial contribution from ohmic heating $E_{\parallel}J_{\parallel}$ at ignition, and a relatively stronger thermal excursion. It was also found[86] that ignition could potentially be achieved at B_T below the design values, if the improved confinement that has been observed to be associated with reversed shear profiles (q profiles with a single minimum in the middle of the plasma radius) could be achieved. Investigation of the higher temperature deuterium-^{3}He fusion reaction also supports the important role of the current ramp. These simulations have found that in general there is only a relatively small range of possible parameters for the optimum current ramp to ignition.

Recently we have also investigated the deuterium-tritium ignition possibilities of a very different configuration. ITER,[87] this proposed fusion experiment, has a much lower toroidal field and current and particle densities. The parameters are R = 8.14 m, a = 2.80 m, with a maximum vertical elongation factor

84   L.E. Sugiyama and W. Park, *A Two-Fluid Model for Toroidal Plasmas*, RLE PTP-96/2 (Cambridge: MIT Research Laboratory of Electronics, 1997); L.E. Sugiyama, "Two-Fluid Toroidal Effects in Tokamak Plasmas," *Proceedings International Workshop on Nonlinear and Extended MHD*, Madison, Wisconsin, 1997, Center for Plasma Theory and Computation Report UW-CPTC 97-5 (Madison, Wisconsin: University of Wisconsin. 1997).

85   B. Coppi, M. Nassi, and L.E. Sugiyama, "Physics Basis for Compact Ignition Experiments," *Phys. Scripta* 45: 112-32 (1992); B. Coppi and the Ignitor Project Group, *J. Fusion Energy* 13: 111 (1994).

86   L.E. Sugiyama, "Reversed Shear Ignition for High Field Tokamaks," *Proceedings of the 23rd European Physical Society Conference on Controlled Fusion and Plasma Physics*, Kiev, Ukraine, 1996.

κ = 1.75 and triangularity δ = 0.24 (for a D-shaped plasma cross-section), maximum toroidal field B_T = 5.7 T, current I_p = 21 MA, and edge q_a = 3. Although it has been widely studied, little has been done on time-dependent ignition. We have taken a fresh approach[88] to try to identify the optimal approach to ignition, using the current ramp for heating as much as possible. As a first step, we assume the most favorable conditions for ignition, keeping in mind that these conditions, particularly the assumption of plasma purity, are unlikely to be met in practice for the relatively low plasma densities involved, and that the optimum ignition approach and parameters change considerably as these conditions degrade. The energy confinement time, which should be as high as possible to reach ignition temperatures easily, also falls with the increased plasma heating that then becomes necessary. The results also establish the optimum current ramp rates and times for the machine. These are in general agreement with previous results.[89] It is also interesting that the general requirement on the minimum energy confinement time required for ignition is found about twice that given by the standard ITER-89P[90] L-mode scaling at ignition, in agreement with previous steady state studies, although the plasma parameters considered here are very different. The τ_E can be smaller before ignition is approached.

A fusion model incorporating all the major reactions from the D-^{3}He fusion cycle was used, with bremsstrahlung and synchrotron radiation models that should be valid to high temperature.

The most favorable conditions for (D-T) ignition consist of a clean, or pure, plasma with the effective ion charge Z_{eff} $\simeq$ 1 and a 50:50 D:T composition. We consider both fusion-produced α-particle accumulation and artificial removal. It is assumed that the maximum parameters are reached at the end of the current ramp. The plasma size and shape, plasma density and fuelling rates, current ramp rates and times, auxiliary heating, are varied over the current ramp interval. The thermal transport diffusion coeffi-

cients are also varied, relative to experimentally determined scalings for the global energy confinement time, to give estimates of the ignition margin. The plasma q is also constrained. Because the plasma breakdown state is not well known, the simulations were started shortly (20 sec) after the initial plasma formation, at an assumed 2 MA of toroidal plasma current and given density. For simplicity, the initial plasma was assumed to be centered at the final R_0, with a circular configuration of half the final horizontal minor radius a. (These parameters are again relatively strongly constrained by the existence of a breakdown magnetic configuration.)

Two current ramps were considered, 200 sec to I_p = 21 MA and 110 sec to I_p = 18 MA, the maximum design current.

The results of the simulations show that, for clean plasmas, using very low plasma densities gives the most efficient ignition, which occurs at very high central temperatures. True ignition, where the fusion power deposited in the plasma balances the plasma power losses, can occur around the end of the long current ramp, 200 sec, with the minimum q $\geq$ 1.1. Good ion energy confinement, which allows central T_{io} almost twice T_{eo}, also favors ignition. Initial central electron densities of 0.3 x 10^{20} m^{-3}, rising to 10^{20} m^{-3}, with volume averages of 0.27 rising to 0.62 (in the same units of 10^{20} m^{-3}) by 200 seconds can reach very high central temperatures of T_{io} $\simeq$ 75 keV and T_{eo} $\simeq$ 54 keV, with volume averages 18 and 13.7 keV, respectively. This corresponds to 300 MW in fusion α-particle power. Auxiliary heating during the current ramp, starting from 24 MW at 60 sec and increasing to 30 MW at 140 sec was used. In addition, the energy confinement times, measured relative to the standard ITER-89P[91] L-mode scaling, ranged from 1.4 at the beginning to about 2 at the end of the ramp. However, these scenarios are unrealistic. The plasma betas are large enough (normalized total betas ($\beta_N = \beta/(I_p/aB_T)$) about 2.5) that severe instability is likely well before this state is reached.

87 R. Aymar, V. Chuyanov, M. Huguet, R. Parker, Y. Shimomura, and the ITER Joint Central Team and Home Teams, "ITER Project: A Physics and Technology Experiment," and accompanying papers, *Proceedings of the 16th International IAEA Conference on Fusion Energy* 2: 737-1002, Montreal, Canada, October 1996 (Vienna, Austria: International Atomic Energy Agency, 1997).

88 M.-H. Kuang, *D-T Ignition in the ITER and Ignitor Experiments*, Senior thesis, Department of Physics, MIT, 1997.

89 S.C. Jardin, C.E. Kessel, and N. Pomphrey, "Poloidal Flux Requirements for the International Thermonuclear Reactor," *Nucl. Fusion* 34(8): 1145-60 (1994).

90 P. Yushmanov, T. Takizuki, K. Riedel, O. Kadaun, J. Cordey, S. Kaye, and D. Post, *Nucl. Fusion* 30: 1999 (1990).

91 Ibid.

A better scenario uses a shorter current ramp 120 sec, to a slightly lower current of 18 MA. In this case, ignition can also be reached, just before the end of the ramp, at lower density (0.7-0.8 central electron, very flat profiles), lower temperatures, and much lower betas. In addition, q_{min} is higher, 1.2 or more and the required τ_E is less, a maximum of 1.8 time L-mode, starting from below 1. The nominally less favorable case, where equal transport between electrons and ions was assumed, had much lower central temperatures at ignition ($T_{io} \simeq 45$ keV, $T_{eo} \simeq 40$ keV with volume averages of about 8 keV, compared to 70 and 39, with volume averages of 10.3 and 7.4, respectively). The q_{min} was also significantly higher, at 1.4. The fusion charged particle powers were approximately 180 MW in both cases, and the normalized total betas ($\beta_N = \beta/(I_p/aB_T)$) were about 1.5 and the poloidal betas about 0.65-0.75. These cases fall below the ITER design point of 300 MW of α-particle power.

The difficulty of trying to ignite with higher densities during the current ramp was also shown. Initial densities of 1.0 (0.87 vol. ave.) increasing to 1.5 (1.0 vol ave.) at 120 sec showed that the major problem is with q_{min}, which drops rapidly during the current ramp because the plasma temperature remains low over most of the plasma. In one example, again using 24 MW of auxiliary heating, starting from 60 sec, ignition was reached at $T_{io} = 23$ and $T_{eo} = 30$ keV at 120 sec, with very low volume averages of 4.6 and 5.0 keV, but q_{min} was already 1.1 (although the central $q_0 = 2.8$).

In summary, this work shows that completely ignited states in a low B_T machine are difficult to attain with a reasonable combination of plasma parameters and plasma stability requirements. Driven burning states, with P_{Fus} less than the plasma power losses, the balance supplied by injected power, have similar problems, particularly with stability. It is shown that for heating and for stability, the necessity of heating during the current ramp phase constrains the possible approach to ignition as well as the final ignition parameters. The constraints favor low-density ignition for ITER. Under plasma conditions that are degraded below those considered here, even more severe constraints will be encountered.

1.2.9 Publications

Journal Articles

Airoldi, A., G. Cenacchi, and B. Coppi. "Fusion Performance of High Magnetic Field Experiments." *Bull. Am. Phys. Soc.* 41(10): 1834 (1997).

Belova, E.V., W. Park, G.Y. Fu, H.R. Strauss, and L.E. Sugiyama. "3D Hybrid Simulations with Gyrokinetic Particle Ions and Fluid Electrons." *Bull Am. Phys. Soc.* 42(10): 1854 (1997).

Bombarda, F., P. Buratti, B. Coppi. "Relevance of Present Reverse Shear Experiments to Ignitor." *Bull. Am. Phys. Soc.* 41(10): 1835 (1997).

Coppi, B., G. Penn, C. Riconda. "Excitation of Contained Modes by High Energy Nuclei and Correlated Cyclotron Emission." *Ann. Phys.* 261(2): 117-62 (1997).

Daughton, W., P. Catto, B. Coppi, and S.I. Krasheninnikov. "Interchange Instabilities in a Partially Ionized Plasma." *Phys. Plasmas.* Forthcoming.

Galas-So, G., L. Lanzavecchia, G. Dalmut, G. Drago, A. Laurenti, R. Marabotto, G. Ghia, G. Munaro, M. Pirozzi, L. Destefanis, R. Andreani, C. Crescenzi, A. Cucchiaro, M. Gasparotto, A. Pizzuto, B. Coppi. "Ignitor Prototype Construction Program." *Bull. Am. Phys. Soc.* 41(10): 1834 (1997).

Park, W., E.V. Belova, G.Y. Fu, H.R. Strauss, L.E. Sugiyama. "M3D (Multi-level 3D) Project for Simulation of Plasmas." *Bull Am. Phys. Soc.* 42(10): 1854 (1997).

Pizzuto, A., G. Mazzone, B. Coppi. "Halo Current Effects on Ignitor Plasma Chamber." *Bull. Am. Phys. Soc.* 41(10): 1834 (1997).

Rice, J.E., M.J. Greenwald, I.H. Hutchinson, E.S. Marmar, Y. Takase, S.M. Wolfe, F. Bombarda. "Observations of Central Toroidal Rotation in ICRF Heated Alcator C-Mod Plasmas." MIT Report PSFC/JA-97-4. Submitted to *Nucl. Fusion.*

Sugiyama, L.E. and W. Park. "Plasma Rotation in Two-Fluid Tokamaks." *Bull Am. Phys. Soc.* 42(10): 1854 (1997).

Conference Papers

Coppi, B. and W.S. Daughton. "Composite Transport Coefficients for Well Confined Plasmas." *Proceedings of the 24th European Physical Society Conference on Controlled Fusion and Plasma Physics*, Berchtesgaden, Germany, June 1997.

Coppi, B., S. Migliuolo, L.E. Sugiyama, F. Bombarda, P. Detragiache. "Evolution of Global Modes and Magnetic Reconnection in Fusion Burning Plasmas." *Proceedings of the 16th International IAEA Conference on Fusion Energy* 2: 397, Montreal, Canada, October 1996 (Vienna, Austria: International Atomic Energy Agency, 1997).

Park, W., G.Y. Fu, H.R. Strauss, L.E. Sugiyama. "3D Simulation Studies of Tokamak Plasmas using MHD and Extended-MHD Models." *Proceedings of the 16th International IAEA Conference on Fusion Energy* 2: 411, Montreal, Canada, October 1996 (Vienna, Austria: International Atomic Energy Agency, 1997).

Park, W., G.Y. Fu, H.R. Strauss, L.E. Sugiyama. *Proceedings Int. Workshop on Nonlinear and Extended MHD*, Madison, Wisconsin, 1997, *Center for Plasma Theory and Computation Report* UW-CPTC 97-5 (Madison, Wisconsin: University of Wisconsin, 1997).

Sugiyama, L.E. "Two-Fluid Toroidal Effects in Tokamak Plasmas." *Proceedings Int. Workshop on Nonlinear and Extended MHD*, Madison, Wisconsin, 1997, Center for Plasma Theory and Computation Report UW-CPTC 97-5 (Madison, Wisconsin: University of Wisconsin, 1997).

Sugiyama, L.E. and W. Park. "Two-Fluid and Parallel Compressibility Effects in Tokamak Plasmas." Invited paper presented at *2nd Asian Plasma Physics and Theory Conference*, Toki, Japan, October 1997. Forthcoming.

Technical Reports

Sugiyama, L.E. and W. Park. *A Two-Fluid Model for Toroidal Plasmas*. RLE PTP-96/2. Cambridge, Massachusetts: MIT Research Laboratory of Electronics, 1997.

Thesis

Daughton, W.S. *Transport Processes in Well Confined High Temperature Plasmas and Collective Modes in their Partially Ionized Edge Region.* Ph.D. diss., Dept. of Physics, MIT, 1998.

Kuang, M.-H. *D-T Ignition in the ITER and Ignitor Experiments.* Senior thesis, Dept. of Physics, MIT, 1997.